(12) INTERNATIONAL APPLICATION PUBLISHED UNDER THE PATENT COOPERATION TREATY (PCT)

(19) World Intellectual Property Organization
International Bureau

(43) International Publication Date
25 September 2014 (25.09.2014)

WIPO | PCT

(10) International Publication Number
WO 2014/149043 A1

(51) International Patent Classification:
G05D 1/00 (2006.01) *G06F 19/00* (2011.01)

(21) International Application Number:
PCT/US2013/033142

(22) International Filing Date:
20 March 2013 (20.03.2013)

(25) Filing Language: English

(26) Publication Language: English

(71) Applicant: **INTERNATIONAL TRUCK INTELLECTUAL PROPERTY COMPANY, LLC** [US/US]; 2701 Navistar Drive, Lisle, Illinois 60532 (US).

(72) Inventors: **CHEN, Cheng**; 2311 Kentucky Ct, Naperville, Illinois 60564 (US). **HUANG, Wei**; 1625 South Michigan Ave, Apt 202, Villa Park, Illinois 60181 (US). **ZHANG, Shusen**; 5740 Walnut Avenue Apt 2A, Downers Grove, Illinois 60516 (US). **TAVARES, Fernando**; 2311 Greenfield Dr., Glenview, Illinois 60025 (US). **SU, Xiaoxin**; 370 Ash Ln #304, Glen Ellyn, Illinois 60137 (US).

(74) Agents: **BACH, Mark** et al.; 2701 Navistar Drive, Lisle, Illinois 60532 (US).

(81) Designated States *(unless otherwise indicated, for every kind of national protection available)*: AE, AG, AL, AM, AO, AT, AU, AZ, BA, BB, BG, BH, BN, BR, BW, BY, BZ, CA, CH, CL, CN, CO, CR, CU, CZ, DE, DK, DM, DO, DZ, EC, EE, EG, ES, FI, GB, GD, GE, GH, GM, GT, HN, HR, HU, ID, IL, IN, IS, JP, KE, KG, KM, KN, KP, KR, KZ, LA, LC, LK, LR, LS, LT, LU, LY, MA, MD, ME, MG, MK, MN, MW, MX, MY, MZ, NA, NG, NI, NO, NZ, OM, PA, PE, PG, PH, PL, PT, QA, RO, RS, RU, RW, SC, SD, SE, SG, SK, SL, SM, ST, SV, SY, TH, TJ, TM, TN, TR, TT, TZ, UA, UG, US, UZ, VC, VN, ZA, ZM, ZW.

(84) Designated States *(unless otherwise indicated, for every kind of regional protection available)*: ARIPO (BW, GH, GM, KE, LR, LS, MW, MZ, NA, RW, SD, SL, SZ, TZ, UG, ZM, ZW), Eurasian (AM, AZ, BY, KG, KZ, RU, TJ, TM), European (AL, AT, BE, BG, CH, CY, CZ, DE, DK, EE, ES, FI, FR, GB, GR, HR, HU, IE, IS, IT, LT, LU, LV, MC, MK, MT, NL, NO, PL, PT, RO, RS, SE, SI, SK, SM, TR), OAPI (BF, BJ, CF, CG, CI, CM, GA, GN, GQ, GW, ML, MR, NE, SN, TD, TG).

Declarations under Rule 4.17:

— *as to the identity of the inventor (Rule 4.17(i))*

— *as to applicant's entitlement to apply for and be granted a patent (Rule 4.17(ii))*

— *of inventorship (Rule 4.17(iv))*

Published:

— *with international search report (Art. 21(3))*

— *with amended claims (Art. 19(1))*

(54) Title: SMART CRUISE CONTROL SYSTEM

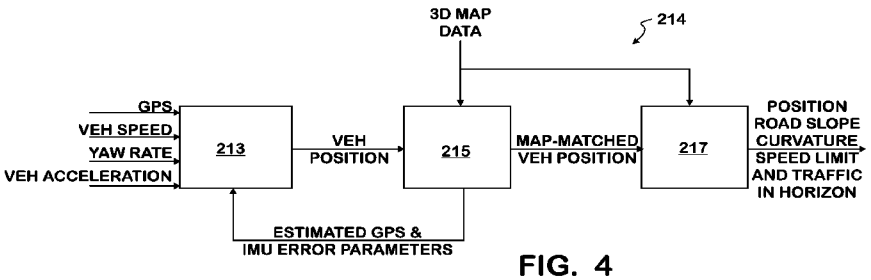

FIG. 4

(57) Abstract: A method and apparatus for controlling the operation of a vehicle using a predictive control system. The technology includes predicting a characteristic of a portion of a road and defining a cost function based on a plurality of vehicle parameters and the predicted road characteristic. Engine torque and engine brake torque commands and vehicle set speed are calculated, and a gear shifting command is determined. The system may include a Kalman filter for estimating vehicle mass and road grade when measurements of a navigation sensor and data from a three dimensional map are unavailable, and a Kalman filter for estimating vehicle mass, aerodynamic drag, and rolling resistance when the navigation sensor measurements and map data are available. The engine torque, engine brake torque, and gear shifting commands are adjusted based on the predicted road characteristic to follow the calculated vehicle set speed to minimize the defined cost function.

WO 2014/149043 A1

SMART CRUISE CONTROL SYSTEM

BACKGROUND

[0001] Longitudinal vehicle control systems, such as, for example, optimal cruise control on the highway, requires accurate model of a vehicle's longitudinal dynamics to achieve desired levels of safety and closed-loop performance. For example, basic models of longitudinal vehicle dynamics are typically built on the assumption that the vehicle is travelling on a road with constant grade. Additionally, other vehicle and operational parameters used to build the model may be unknown and/or vary during usage of the vehicle. Accordingly, variances in operational parameters that are encountered during vehicle usage, such as changes in road grade, among other parameters, often limit the accuracy of such models. Thus, as these models may not account for at least some variances in operational parameters, the performance of the associated control system may be adversely impacted. Moreover, such variances or unknown parameters may prohibit control systems based on such models from attaining optimal performance during at least some periods of vehicle usage. Accordingly, at least some system models may attempt to identify particular vehicle parameters while the vehicle is in operation.

[0002] Two operational parameters that are typically of interest for longitudinal vehicle control systems are vehicle mass and road grade. However, in use, the mass due to the load of a heavy-duty vehicle can, for example, increase by around 400%. Accordingly, some vehicles are equipped with pneumatic suspension and electronically controlled suspension (ECS) that are able to measure the vehicle's mass directly through air pressure. However, this configuration is not present in all vehicles. With respect to road grade, some vehicles may employ an active global positioning system (GPS) and/or road inclination sensor to indirectly or directly measure the current road grade. Yet, the GPS signal may be ineffective or become corrupted, such as, for example, because the GPS is not activated or not connected to an adequate number of satellites, or the GPS map is inaccurate.

[0003] Algorithms used for longitudinal vehicle dynamics models typically assume that the vehicle is travelling on a road with instantaneous constant grade. Further,

existing algorithms often require certain measurement mechanisms, such as GPS or an inertial sensor, to indirectly infer the road grade. Further, such algorithms are typically based on the linearization of a nonlinear system and require prior knowledge of measurement noise statistical characteristics.

[0004] Additionally, typically, conventional cruise control attempts to maintain vehicle speed at a desired value by adjusting the throttle command. However, conventional cruise control typically does not take into account environmental parameters, such as, for example, road gradient and road curvature, which could induce safety issues and necessitate driver intervention. As a result, some cruise control systems implement predictive speed control systems. However, predictive speed control systems, in their optimal control, typically have only two inputs, namely the throttle pedal position and an engine brake, or service brake, signal. Further, gear shifting is taken care of by a transmission controller. This characteristic however may make the optimal control sub-optimal, or even not optimal, when the transmission controller is not tuned properly for the current vehicle configuration.

[0005] Further, to do all of the optimization, predictive speed control systems may require exact knowledge of major vehicle parameters. Thus, for example, a major parameter changes during operation of the vehicle, such as when the weight of the vehicle changes, and those changes are not reflected in the optimization algorithm, the optimized control input may no longer be optimized. Similarly, for example, the optimized control input may also no longer be optimized when the speed and direction of the wind changes, or road surface roughness and tire inflation condition changes the rolling resistance of the tire.

SUMMARY

[0006] Certain embodiments of the present technology provide a method for controlling operation of a vehicle that is traveling along a road using an adaptive control system. The method includes estimating a road curvature in a vertical plan of the road. The method also includes providing the predicted road curvature to a vehicle parameter estimation block, the vehicle parameter estimation block having a first Kalman filter and a second Kalman filter. Additionally, when available, a navigational signal is provided to

the second Kalman filter, the navigational signal providing information regarding a characteristic of a portion of the road on the horizon. Further, when the navigational signal is unavailable, the first Kalman filter estimates a first set of vehicle parameters. The method also includes estimating by the second Kalman filter, when the navigational signal is available, a second set of vehicle parameters.

[0007] Additionally, certain embodiments of the present technology provide a method for controlling operation of a vehicle system that is traveling along a road using an adaptive control system using a Kalman filter having a first sub-Kalman filter and a second sub-Kalman filter. The method includes estimating by the first sub-Kalman filter a plurality of state estimations and estimating by the second sub-Kalman filter a plurality of parameter estimations. Further, the plurality of state estimations are communicated to the second sub-Kalman filter and the plurality of parameter estimations are communicated to the first sub-Kalman filter. The method also includes utilizing an inherited nonlinear model of the vehicle to construct a nonlinear states transformation and a nonlinear input transformation and feeding back the nonlinear states transformation and the nonlinear input transformation to linearize the vehicle system. The method also incudes stabilizing the linearized vehicle system at an arbitrary position in a state space.

[0008] Certain embodiments of the present technology also provide a method for controlling operation of a vehicle system that is traveling along a road using an adaptive control system. The method includes estimating a road curvature in a vertical plane of the road and estimating, by a Kalman filter, a plurality of state estimations and a plurality of parameter estimations. The method also includes utilizing an inherited nonlinear model of the vehicle to construct a nonlinear states transformation and a nonlinear input transformation. The method also includes feeding back the nonlinear states transformation and nonlinear input transformation to linearize the vehicle system and stabilizing the linearized system at an arbitrary position in a state space.

[0009] Certain embodiments of the present technology provide a method for controlling the operation of a vehicle that has a transmission and an engine using a predictive control system. The method includes predicting a characteristic of a portion of the road and defining a cost function based on a plurality of vehicle parameters and the predicted characteristic the road. Further, the method includes calculating, based at least

in part on the predicted road characteristic and on minimizing the defined cost function, an engine torque command and an engine brake torque command for the operation of the engine, and a vehicle set speed. Additionally, the method includes determining, based at least in part on the predicted road characteristic and on minimizing the defined cost function, a gear shifting command for operation of the transmission and transmitting a signal representative of the gear shifting command to an electronic control unit associated with the transmission. The method also includes adjusting the engine torque command, the engine brake torque command, and the gear shifting command based on the predicted road characteristic to follow the calculated vehicle set speed to minimize the defined cost function.

[0010] Certain embodiments of the present technology also provide a method for controlling the operation of a vehicle having an engine using a predictive control system. The method includes predicting a characteristic of a portion of the road and measuring by a radar system at least one radar measurement between the vehicle and another vehicle and defining a cost function based on a plurality of vehicle parameters, the predicted road characteristic, and the at least one radar measurement. The method also includes calculating, based at least in part on the predicted road characteristic and on minimizing the defined cost function, an engine torque command for the operation of the engine and a vehicle set speed. Additionally, the method includes adjusting the engine torque command based on the predicted road characteristic and the at least one radar measurement to follow the calculated vehicle set speed to minimize the defined cost function, and to maintain a safe distance between the vehicle and another vehicle.

[0011] Additionally, certain embodiments of the present technology provide a method for controlling the operation of a vehicle using a predictive control system. The method includes predicting a characteristic of a portion of the road and measuring by a radar system at least one radar measurement between the vehicle and another vehicle. The method further includes calculating, based at least in part on the predicted road characteristic and the at least one radar measurement, an engine torque command for the operation of the engine and a vehicle set speed.

[0012] Further, certain embodiments of the present technology provide an apparatus for controlling the operation of a vehicle using a predictive control system. The

apparatus includes a vehicle positioning and horizon generation system configured to receive data from a Global Positioning System, an inertial measurement unit, and a three dimensional map database, and to generate a road characteristic signal. The apparatus also includes an adaptive optimal control system configured to receive the road characteristic signal and a parameter estimation signal. The adaptive optimal control system has a first Kalman filter and a second Kalman filter. The first Kalman filter configured to estimate a vehicle mass and a road grade when the navigation sensor measurements and data from the three dimensional map database are not available. The second Kalman filter is configured to estimate vehicle mass, aerodynamic drag, and rolling resistance when the navigation sensor measurements and data from the three dimensional map database are available. The apparatus also includes a vehicle parameter estimator block configured to receive the road characteristic signal, a sensed data from a vehicle states sensor, and a control input signal, and generate a parameter estimation signal that provides an estimate of at least one of the adjustable parameters: vehicle mass, aerodynamic drag, and rolling resistance. Additionally, the apparatus includes a nonlinear adaptive cruise controller configured to provide a control input signal based at least in part on the parameter estimation signal, the states and weight estimates, and the vehicle states sensor. The nonlinear adaptive cruise controller includes a plurality of nonlinear states transformation blocks and a nonlinear inputs transformation block. The control input signal configured to provide instructions for the operation of an engine and a transmission of the vehicle.

[0013] Further, certain embodiments of the present technology provide an apparatus for controlling the operation of a vehicle using a predictive control system. The apparatus includes a vehicle positioning and horizon generation system configured to receive data from a Global Positioning System, an inertial measurement unit, and a three dimensional map database, and to generate a road characteristic signal. The apparatus also includes an adaptive optimal control system configured to receive the road characteristic signal and a parameter estimation signal, the adaptive optimal control system having a first Kalman filter and a second Kalman filter, the first Kalman filter being configured to estimate a vehicle mass and a road grade when navigation sensor measurements and the map data are not available. The second Kalman filter is configured

to estimate vehicle mass, aerodynamic drag, and rolling resistance when the navigation sensor measurements and the map data are available. The apparatus also includes a vehicle parameter estimator block configured to receive the road characteristic signal, a sensed data from a vehicle states sensor, and a control input signal, and generate a parameter estimation signal that provides an estimate of at least one of the adjustable parameters: vehicle mass, aerodynamic drag, and rolling resistance. Additionally, the apparatus includes a radar system having at least one radar, the radar system configured to provide a radar measurement reflecting the distance between the vehicle and another vehicle. Further, the apparatus includes a nonlinear adaptive cruise controller configured to provide a control input signal based at least in part on the parameter estimation signal, the states and weight estimates, and the vehicle states sensor, and the radar measurement. The nonlinear adaptive cruise controller includes a plurality of nonlinear states transformation blocks and a nonlinear inputs transformation block. The control input signal is configured to provide instructions for the operation of an engine and a transmission of the vehicle.

BRIEF DESCRIPTION OF THE DRAWINGS

[0014] Figure 1 illustrates a comparison of the performance of a conventional cruise control strategy and the smart cruise control strategy of the illustrated technology for a vehicle that is traveling along a road that includes an incline in road slope.

[0015] Figure 2 illustrates a comparison of the performance of a conventional cruise control strategy and the smart cruise control strategy of the illustrated technology for a vehicle that is traveling along a road that includes a decline in road slope.

[0016] Figure 3 illustrates a block diagram of a smart cruise control system according to an illustrated embodiment.

[0017] Figure 4 illustrates a vehicle positioning and horizon generation system according to an illustrated embodiment.

[0018] Figure 5 illustrates a block diagram of a Kalman filter that includes an extended Kalman state filter and an extended Kalman weight filter.

[0019] Figure 6 illustrates an adaptive optimal control system according to an illustrated embodiment.

[0020] Figure 7 illustrates a longitudinal free body diagram.

[0021] Figure 8 illustrates a comparison of real and approximated engine map.

[0022] Figure 9 illustrates a comparison of real and approximated brake specific fuel consumption time rate map.

[0023] Figure 10 illustrates a complete SQP algorithm flow chart.

[0024] Figure 11 illustrates a nonlinear adaptive cruise controller according to an illustrated embodiment.

[0025] Figure 12 illustrates architecture of a feedback control system.

[0026] Figure 13 illustrates a Linear Quadratic Gaussian/Linear Quadratic Regulator set point control.

[0027] Figure 14 illustrates a vehicle parameter estimation block according to an illustrated embodiment.

[0028] Figure 15 illustrates parameterized torque curves.

[0029] Figure 16 illustrates data from two simulation tests of the normal mode unscented Kalman filter.

[0030] Figure 17 illustrates a vehicle at three different locations along a road.

[0031] Figure 18 illustrates the planner dynamics of a vehicle that is on an inclined and curved road.

[0032] Figure 19 illustrates a simulation of road grade in which the Kalman filter is an unscented Kalman filter, and in which the perfect noise free measurement is assumed.

[0033] Figure 20 illustrates a simulation of vehicle mass in which the Kalman filter is an unscented Kalman filter, and in which the perfect noise free measurement is assumed.

[0034] Figure 21 illustrates a block diagram of an embodiment of a smart cruise control platform that uses a prototyping laptop to control one or more electronic control units of a vehicle.

[0035] Figure 22 illustrates a block diagram of an embodiment of a smart cruise control platform that uses an electronic control module to control one or more electronic control units of a vehicle.

[0036] Figure 23 illustrates a first vehicle that is in the horizon of a second vehicle and in which information may be exchanged between the smart cruise control systems of both vehicles.

[0037] Figure 24 illustrates a radar enabled cruise control system according to an illustrated embodiment.

[0038] Figure 25 illustrates a block diagram of a radar enabled cruise control platform according to an illustrated embodiment.

DETAILED DESCRIPTION

[0039] Figure 1 illustrates a comparison of the performance of a conventional cruise control strategy and the smart cruise control strategy of the illustrated technology. As shown in at least the top portion of Figure 1, a vehicle 200 is illustrated as traveling along a relatively flat stretch of road from a distance of 1640 feet (ft) to 4250 ft and at an altitude of 0 ft. The vehicle 200 is shown to then proceed to an inclined portion of the road from 4250 ft to 7550 ft, during which the vehicle 200 climbs from an altitude of 0 ft to 66 ft. After reaching the end of the incline, the vehicle 200 resumes traveling along a relatively flat stretch of road from a distance of 7550 ft to 11480 ft at an altitude of 66 ft.

[0040] In the example illustrated in Figure 1, the vehicle 200 is traveling at a set speed point of 56 miles-per-hour (mph). According to certain embodiments, the smart cruise control strategy of the present technology varies the set speed of the vehicle 200 according to information regarding the terrain or characteristics of the upcoming road, or in the horizon, that the vehicle 200 approaching. More specifically, the smart cruise control strategy may examine the conditions of upcoming terrain, such as, for example, whether a vehicle 200 is approaching a portion of the road in which the slope and/or

curvature of the road changes. According to certain embodiments, the smart cruise control strategy may also examine the degree and/or length of such a slope and/or curvature, and/or the differences between the slope and/or curvature of the portion of the road that the vehicle 200 is currently on and the portion of the road in the horizon that the vehicle 200 is approaching.

[0041] Using information regarding the upcoming terrain, the smart cruise control strategy may adjust an operating parameter of the vehicle 200 before the vehicle encounters a change in terrain. For example, referencing Figure 1, by estimating that the vehicle 200 is approaching an increase in the slope of the road, the smart cruise control strategy may increase the speed of the vehicle 200 while the vehicle 200 is still on the relatively flat portion of road, and before the vehicle 200 reaches the start of the incline at the 4250 ft marker. Moreover, in the embodiment shown in Figure 1, the speed of the vehicle 200 is shown as starting to increase from 56 mph before the vehicle 200 reaches the 4250 ft marker, and reaches a peak speed at about the time the vehicle 200 begins the incline at the 4250 ft marker. Conversely, the conventional cruise control strategy is shown as maintaining a constant set speed of 56 mph until the vehicle 200 begins traveling along the incline.

[0042] By varying, and more specifically, by increasing, the set speed point before the vehicle 200 begins the incline, the vehicle 200 using the smart cruise control strategy may enter the incline with sufficient speed to allow the vehicle 200 to at least initially travel at a sufficient speed along the incline without the need to operate the accelerator over the entire incline as required by conventional cruise control strategy and thus reduce the associated usage of fuel. Additionally, by accelerating the speed of the vehicle 200 before the vehicle 200 enters the incline, compared to a vehicle being operated by conventional cruise control strategy, the vehicle 200 may travel at least a portion of the incline before the speed of the vehicle 200 drops back down to the set point. Thus, for certain road conditions, the vehicle 200 using the smart cruise control strategy may travel a relatively larger portion of the incline, or have a relatively shorter portion of the incline remaining, than a vehicle being operated by conventional cruise control before downshifting of the transmission gearing may be activated. Further, under certain conditions, the smart cruise control strategy may allow for the vehicle 200 to

travel along an incline without the need for downshifting. By reducing or eliminating the need for such downshifting and upshifting, the smart cruise control strategy may allow for a potential reduction in wear on the transmission and associated transmission components, and an associated usage of fuel. Conversely, the speed of the vehicle 200 using conventional cruise control strategy may, as illustrated in Figure 1, drop below the set point as the vehicle 200 initially begins traveling up the incline. Accordingly, the vehicle 200 using a conventional cruise control strategy may travel a relatively short distance along the incline and/or have a relatively long portion of the incline remaining, when the speed of the vehicle 200 drops to a level that results in downshifting of the transmission.

[0043] Figure 2 illustrates a comparison of the performance of conventional cruise control strategy and the smart cruise control strategy of the illustrated technology for a vehicle 200 that is traveling along a road that includes a decline in road slope. As shown between distances 1640 ft and 3610 ft, the vehicle 200 is traveling along a relatively flat road at an altitude of 0 ft. Then, between distances 3610 ft and 6890 ft, the vehicle 200 travels along a decline that drops from an altitude of 0 ft to -131.2 ft. Next, between distances 6890 ft and 11480 ft, the vehicle 200 resumes traveling along a relatively flat road but at a lower altitude of -131.2 ft.

[0044] As shown in Figure 2, while still on the flat portion of road, the smart cruise control strategy may become aware of the upcoming decline that is in the horizon. Accordingly, the smart cruise control strategy may reduce the speed of the vehicle 200 before the vehicle 200 begins the descent down the decline. The subsequent loss in speed experienced on the flat portion of the road may subsequently be regained while the vehicle 200 travels along the decline, where the vehicle 200 regains speed by converting the potential energy to kinetic energy. This decrease in speed while on a flat portion of road may translate into a reduced amount of fuel being consumed by the vehicle 200 when compared with associated set speed being maintained by the vehicle 200 that is being operated with conventional cruise control strategy. Additionally, the reduced speed of the vehicle 200 that is being operated using the smart cruise control strategy may also minimize the use, and associated wear, of the brakes of the vehicle 200 on the decline when compared to the faster speed at which the vehicle 200 being operated with

conventional cruise control strategy begins the decline. Moreover, as the vehicle using the conventional cruise control strategy may attain the top speed of 61 faster, and need to maintain that speed longer, than the vehicle 200 that is being operated with the smart cruise control strategy, and thereby require use of the braking system for a longer period of time. Thus, the strategy of the smart cruise control may allow for shorter and less intense braking than achieved by the vehicle 200 that is employing the conventional cruise control strategy.

[0045] Figure 3 illustrates a block diagram of a smart cruise control system 210 for a motor vehicle, which minimizes vehicle operating costs based on information regarding upcoming road terrain, estimated vehicle parameters, and traffic information. The smart cruise control system 210 is configured to provide coordinated optimal control of throttle position and brake and gear shifting while the vehicle 200 is operating in cruise control. According to certain embodiments, the smart cruise control system 210 includes one or more navigation sensors 212, such as a Global Positioning System (GPS) and a Inertial Measurement Unit (IMU), that are configured to receive the location, position, and/or path of travel of the vehicle 200. The smart cruise control system 210 may also include and/or have access to a three-dimensional map or terrain database 211, such as a commercially available three-dimensional map, that contains information pertaining to the road, such as the slope, curvature, shape, and orientation, speed limit, and the real time and historical traffic conditions, among other information. Such three-dimensional map data, and well as positional information from the navigation sensors 212, may be used by the smart cruise control system 210 in estimating the terrain that the vehicle 200 is approaching. Additionally, the smart cruise control system 210 may also include vehicle states sensors, such as, for example, sensors that provide information regarding engine speed and wheel speed, among other sensors, with the output of those sensors being indicated by "Veh States Sensor outputs" in Figure 3.

[0046] Figure 4 illustrates a vehicle positioning and horizon generation system 214 according to an illustrated embodiment. As shown, the sensor fusion system 213 may combine information from different navigation sensors 212, such as, for example, GPS, odometer, gyroscope, and accelerometer, to determine the accurate and robust vehicle current position. The sensor fusion system 213 may increase the precision of

determining the position of the vehicle 200, as well as enable dead reckoning navigation when signals from the GPS are unavailable, as discussed below. Further, the vehicle 200 current position and the three-dimensional map or terrain database 211, such as street network and elevation, are fed to a map matching system 215 to calculate the exact map-matched car position. This may be accomplished by using a map matching algorithm that uses both geometric and topological information to increase the precision of vehicle position estimation by matching raw positional data against the road network. The map matching system 215 may further improve the accuracy and robustness of the position estimation in the sensor fusion system 213 by feeding back to the sensor fusion system 213 estimated GPS and IMU sensor error parameters from the map matching system 215. Such feedback to the sensor fusion system 213 may allow the sensor fusion system 213 to attribute for possible errors in GPS and IMU sensed data, and thereby improve the accuracy of the resulting vehicle position information being relied upon by the map matching system 215.

[0047] Further, information from the map-matching system 215 is provided to the horizon generation system block 217. The horizon generation system block 217 may also store or receive data from a three-dimensional map database. Using information provided to and/or stored by the horizon generation system block 217 may allow the horizon generation system block 217 to form and provide the data structure describing the terrain of the upcoming road, also referred to as the road in the horizon. Such information provided by the horizon generation system block 217 may include, but is not limited to, the position or location of the vehicle, the slope and curvature of the road, the speed limit(s), and the real time and historical traffic conditions, in the horizon. In the event a GPS signal from the GPS is not available to the sensor fusion system 213 but the terrain map is available to the map matching system 215, the location of the vehicle 200 may be determined by dead reckoning navigation and map matching. During dead reckoning navigation, the current and/or upcoming position of the vehicle 200 and the associated terrain may be calculated by use of a previously determined position and advancing that position based upon known or estimated speeds over elapsed time, and against the road network.

[0048] The position of the vehicle 200 and the road profile and curvature in the horizon from the vehicle positioning and horizon generation system 214 may be fed to an adaptive optimal control system 216 of the smart cruise control system 210. Figure 6 illustrates an adaptive optimal control system 216 according to the illustrated embodiment. The adaptive optimal control system 216, and more specifically, a nonlinear optimization block 218, may receive information from the vehicle positioning and horizon generation system 214, such as, for example, information regarding the position of the vehicle 200 and the current and/or upcoming terrain, such as, for example, the slope and curvature of the road in the horizon, among other information.

[0049] Additionally, during use of the vehicle 200, the desired vehicle inputs and states for operation of the vehicle 200 may be based on the current vehicle 200 location. For example, the nonlinear optimization block 218 may receive information regarding usage constrains, such as real time and historical traffic conditions and speed limit(s), which are sent from the vehicle positioning and horizon generation system, as the part of the information in the horizon, to increase safety of the smart cruise control strategy, such as preventing speeding and collisions with slower vehicles. Additionally, the nonlinear optimization block 218 may receive vehicle parameter estimations, such as, for example, an estimated vehicle mass, aerodynamic drag, and rolling resistance, which may, according to certain embodiments, be provided based on the sensor inputs. Such vehicle parameter estimations may be used by the nonlinear optimization block 218 to facilitate the implementation of the smart cruise control strategy on a variety of vehicles 200 and driving situations. Thus, for example, if the weight of the vehicle 200 changes, this change in weight may be reflected in the nonlinear optimization block 218, while the smart cruise control system 210 is still able to control the vehicle 200 to gain the best fuel economy. Similarly, for example, the nonlinear optimization block 218 may also determine the most optimal control inputs when the speed and direction of the wind changes, or road surface roughness and tire inflation condition changes the rolling resistance of the tire.

[0050] Using information provided to the nonlinear optimization block 218, the nonlinear optimization block 218 may utilize a nonlinear optimization algorithm to determine and/or update the optimal control inputs for the vehicle 200. For example, the

nonlinear optimization block 218 may provide calculations for vehicle speed, throttle position, engine torque command, engine brake command, and transmission gear position, among others. According to certain embodiments, these optimal control inputs may be received by a multiplexer (mux) 220, before being forwarded to, and stored in, a look-up table 222.

[0051] With respect to the nonlinear optimization algorithm, the particular algorithm may vary depending on the characteristics of the vehicle. For example, for a Class 8 truck in which the longitudinal model includes the engine, driveline, wheel, and truck dynamics, but not a tire model (a no-slip condition is assumed), the developed model is derived using the equation of motion for the free body diagram as shown in Figure 7 and Eq. 1.

$$m\frac{dv}{dt} = F_w - F_s - F_{rr} - F_a \qquad \text{(Eq. 1)}$$

[0052] where Fw is wheel drive force, Fs is longitudinal force due to the road grade, $F\gamma\gamma$ is rolling resistance force, and Fa is air drag force:

$$\begin{aligned} F_s &= mg\sin\phi \\ F_{rr} &= C_{rr}mgcos\phi \\ F_a &= 0.5\rho C_d A_{fr}(v - v_{wind})^2 \end{aligned} \qquad \text{(Eq. 2)}$$

where ϕ is road grade, $C\gamma\gamma$ is rolling resistance coefficient, ρ is air density, Cd is aerodynamic drag coefficient, $A_{f\gamma}$ is truck frontal area, v is truck velocity, and v_{wind} is wind speed. In this work, $C\gamma\gamma$, ρ, and Cd can be estimated from the vehicle parameter estimator block 244, and real-time v_{wind} can be obtained either from a low-cost anemometer or internet database.

[0053] The engine model may be designed based on a rectangular engine map. The maximum engine torque may be approximated as a function of the engine speed, ω_e. The comparison of real and approximated engine map is shown in Figure 8. With a normalized throttle position u, the transient engine torque can be calculated from

$$\begin{aligned} T_m &= c_1\omega_e^3 + c_2\omega_e^2 + c_3\omega + c_4 \\ T_e &= T_m u - T_{fri} \end{aligned} \qquad \text{(Eq. 3a, b)}$$

where T_m, T_e, and T_{fri} are engine maximum, transient, and friction torque. T_{fri} is calculated based on engine speed ω_e. Coefficients c_1 to c_4 are calculated from a curve fitting.

[0054] The truck fuel consumption may be calculated depending on a modified Brake Specific Fuel Consumption (BSFC) map as shown in Figure 9. The fuel consumption position rate can be approximated as a continuous function of engine speed and power *P,* shown in Eq. 4.

$$\frac{dm_f}{dp} = \frac{1}{v}(b_1\omega_e^4 P + b_2\omega_e^3 P + b_3\omega_e^2 P + b_4\omega_e P + b_5 P) \quad \text{(Eq. 4)}$$

where b_1 to b_5 are coefficients, and p is the position. Engine power P (kw) can be calculated from T_e and ω_e by

$$P = \frac{2\pi T_e \omega_e}{60000} \quad \text{(Eq. 5)}$$

[0055] If the engine, transmission, final drive, and the wheel are considered together with the longitudinal forces, a complete truck longitudinal model differentiated with respect to position is:

$$\frac{dv}{dp} = \frac{1}{v} \cdot \frac{1}{J_w + mr^2 + \eta_d n_d^2 \eta_t n_t^2 J_e}(\eta_d n_d \eta_t n_t T_e - F_s r - F_{rr} r - F_a r - T_b) \quad \text{(Eq. 6)}$$

[0056] where J_w and J_e are the engine and wheel inertia (kg-m^2). η_d, n_d, η_t, and n_t are the efficiency and ratio of transmission and final drive, respectively. r is the wheel radius and T_b is the brake torque, which is determined by the normalized brake input b, and maximum engine brake torque T_{bm} as $T_b = bT_{bm}$.

[0057] The nonlinear optimization algorithm attempts to find a constrained minimum of a nonlinear scalar function of several variables, e.g., truck throttle command u, gear shift g, brake command b, and speed v, based on the road slope/curvature, the speed limit(s), the wind speed, and the estimated vehicle mass, aerodynamic drag, and rolling resistance.

[0058] A general nonlinear optimization problem is described in Eq. 7.

$$\begin{aligned} &\min f(x) \\ &\text{subject to } c_i(x) = 0, \quad i = 1,\dots q \\ &\qquad g_j(x) \le 0, \quad j = 1,\dots,m \\ &\qquad x_{iL} \le x_i \le x_{iU}, \; i = 1,\dots n \end{aligned} \tag{Eq. 7}$$

where f, c, and g are the objective, equality constraint, and inequality constraint functions respectively, x_{iL} and x_{iU} are lower and upper bounds for the variable x_i, and q, m, and n are the number of equality constraints, inequality constraints, and design variables, respectively. The functions f and c are twice continuously differentiable in this work.

[0059] According to such an embodiment, an approximated numerical solution is obtained for the nonlinear optimization problem by discretizing the states and control inputs in each prediction road horizon (L = 3000 m) into a set of step points ($s = L/h$ = 60), with the step distance (h = 50 m). Thus, each prediction horizon may be broken into smaller position intervals as: $p = \{p_1, p_2, \dots p_s\}$. Subsequently, the problem is searching for the parameter vector including the number of $4s$ state and control inputs at the grid points such as, $x = \{u_1, g_1, b_1, v_1, u_2, g_2, b_2, v_2, \dots u_s, g_s, b_s, v_s\}$ that minimize the objective function subject to specified constraints.

[0060] After the number of $4s$ (s is the number of step points) state and control inputs are initialized, the objective function $f(x)$, which is the sum of fuel consumption and travel time as shown in Eq. 8, also referred to as a cost function, is evaluated using Euler's numerical integration method with the step length h along the state and control vectors of Eqs. 4 and 6:

$$f(x) = J_{fuel} + J_{time} + J_{gear} \quad \text{(Eq. 8)}$$

$$J_{fuel} = Qh\sum_{k=1}^{s-1}\frac{1}{v_k}\frac{dm_f}{dp} \quad \text{(Eq. 9)}$$

$$J_{time} = Rh\sum_{k=1}^{s-1}\frac{1}{v_k} \quad \text{(Eq. 10)}$$

$$J_{gear} = O\sum_{k=1}^{s-1}|g_k - g_{k-1}| \quad \text{(Eq. 11)}$$

$$subject\ to\ c_k(x) = v_{k+1} - v_k - h\frac{dv_k}{dp} = 0 \quad \text{(Eq. 12)}$$

where J_{gear} is used to used to eliminate the frequent gear shifting between neighboring grid points. Weighting factors *Q*, *R*, and *O* are currently determined by steady state model analysis to weight fuel consumption more than travel time and gear shifting penalty. The nonlinear equality constraint Eq. 12 is obtained from the vehicle dynamic model in Eq. 6. Additionally, the lower and upper bounds for the control variable *u*, *g*, *b*, *and v* are defined by: $0 \le u \le 1,\ 1 \le g \le 10,\ 0 \le b \le 1,\ v_l \le v \le v_u$, where v_l and v_u are the lower and upper speed bounds.

[0061] The gear shifting is calculated in terms of the change of η_t and n_t the efficiency and ratio of transmission. Additionally, J_{gear} in Eq. 11 is designed to eliminate the frequent gear shifting, which is the change of gear number *g*, between neighboring grid points. After the truck throttle command *u* is calculated, the engine torque command *Te* can be determined based on the throttle command using Eq. 3b ($T_e = T_m u - T_{fri}$.) Engine torque command *Te* may be transmitted via the CAN network as the engine torque override command to control the operation of the engine.

[0062] For the nonlinear optimization problem as described in Eqs. 8 to 12 a standard Sequential Quadratic Programming (SQP) method is employed to find the optimum in the design space. The gradient based algorithm SQP is a procedure that generates iterative converging to a solution of the problem by solving the quadratic approximations to the nonlinear optimization problem. The solution flow chart of the SQP algorithm is illustrated in Figure 10.

[0063] Information from the adaptive optimal control system 216 may then be passed to a multiplexer (mux) 230 before passing onto a nonlinear adaptive cruise controller 232. Figure 11 illustrates a nonlinear adaptive cruise controller 232 according to the illustrated embodiment.

[0064] **I. Degenerate Mode Joint Unscented Kalman Filter**

[0065] The joint estimation by the vehicle parameter estimator block 244 using the control inputs and states inputs ensures that the vehicle parameter estimation provided by the vehicle parameter estimator block 244 is not biased when the vehicle 200 states measurements are corrupted by noise. And even severe cases, such as when the vehicle positioning and horizon generation system 214 is not working, the vehicle parameter estimator block 244 may switch from the normal mode to a degenerated mode, in which a Kalman filter 246b, such as, for example a joint or dual unscented or extended Kalman filter may still estimate the vehicle mass and the road grade. According to certain embodiments, the Kalman filter 246b may operate in the degenerated mode when the vehicle 200 is not in smart cruise control mode and the vehicle positioning and horizon generation system 214 is not turned on. Kalman filter 246b may also operate in the degenerated mode when the terrain map data is not available for some section of road but GPS signal is working properly. In this case the normal mode smart cruise control is not possible because the road profile is not available.

[0066] Under such conditions, the Kalman filter 246b will provide extra training time for the parameter vehicle 200 mass before the smart cruise control system starts. Training time may occur when road profile is not available, but will become available at a later time so that the vehicle positioning and horizon generation system 214 is functional in a degenerate mode rather than a normal mode. In such a situation, the degenerated mode will provide some pre-full mode training time, to gather useful information. Such time and training may improve the accuracy of the initial guess of the mass or weight of the vehicle 200 so that the initial guess is closer to the actual weight or mass value, which may, as previously discussed, may expedite the convergence of the algorithm to the actual weight when the vehicle positioning and horizon generation system 214 becomes functional and the algorithm is in normal mode.

[0067] **Kalman Filter**

[0068] Measurements made during usage of the vehicle 200, such as by sensors, for example, may be made on a continuous or regular basis, such as at predetermined intervals. However, such measurements may lead to the accumulation of a relatively large collection of data, which may contain measurement noise or variations, as well as inaccuracies. For example, the torque value reported by a vehicle CAN bus or vector CAN hardware may be different than the real engine torque signal due to noise, as the engine torque is not measured directly. Instead, it may be a calculated as steady state value from an Engine Control Unit. The real engine torque will be different because the transient effect in the combustion.

[0069] Accordingly, rather than relying on a single measurement from this collection of data, according to certain embodiments, the system may employ a Kalman filter. The Kalman filter may be an algorithm that uses a series of measurements that were taken over a period of time to produce a statistically optimal estimate.

[0070] The general steps of a sequential Kalman filter based on recursive estimation include: using previous posterior estimation of states and covariance and the nominal plant model to estimate a priori estimation of states and covariance of the next step; using the priori estimation of covariance to calculate the Kalman filter gain matrix; and, using the Kalman filter gain and priori estimation of states and covariance to estimate the posterior estimation of states and covariance.

[0071] As shown below, various types of Kalman filters 246b may be employed. Further, according to certain embodiments, the Kalman filter 246b may be an extended Kalman filter that is used to estimate the states of a nonlinear dynamic system. Additionally, according to embodiments in which the Kalman filter 246b is being used to estimate the weight of the vehicle 200, the Kalman filter 246b may be an extended Kalman weight filter that is used to estimate the weights of a nonlinear dynamic system.

[0072] The below equations for the various Kalman filters have the following nomenclature; (1) a bold character identifies a non-scalar variable; (2) a caret means the variable is an estimated value; and (3) a minus sign in the superscript identifies a priori estimation.

[0073] **Linear Kalman Filter**

[0074] A linear Kalman filter may be used to estimate the states linear dynamic system. For example, for a linear discrete time system

$$\begin{aligned}\mathbf{x}_k &= \mathbf{A}\mathbf{x}_{k-1} + \mathbf{B}\mathbf{u}_{k-1} + \mathbf{B}_v\mathbf{v}_k,\\ \mathbf{y}_k &= \mathbf{C}\mathbf{x}_k + \mathbf{n}_k,\end{aligned} \qquad \text{(Eqs. 13a, b)}$$

where **A**, **B**, and **C** are every possible parameters that describes the system, **x** is states, **y** is measurements, and $\mathbf{v}_k$ and $\mathbf{n}_k$ are random signals which describe disturbance and measurement noise. A linear Kalman Filter equations start with initializing

$$\begin{aligned}\hat{\mathbf{x}}_0 &= E[\mathbf{x}],\\ \mathbf{P} &= E\left[(\mathbf{x}_0 - \hat{\mathbf{x}}_0)(\mathbf{x}_0 - \hat{\mathbf{x}}_0)^T\right].\end{aligned} \qquad \text{(Eqs. 14a, b)}$$

where **P** is error covariance, E is expectation, and T is transpose.

[0075] For $k \in \{1, \cdots, \infty\}$, the time update equation of the Kalman filter is

$$\begin{aligned}\hat{\mathbf{x}}_k^- &= \mathbf{A}\hat{\mathbf{x}}_{k-1} + \mathbf{B}\mathbf{u}_{k-1},\\ \mathbf{P}_k^- &= \mathbf{A}\mathbf{P}_{k-1}\mathbf{A}^T + \mathbf{B}_v\sigma_v^2\mathbf{B}_v.\end{aligned} \qquad \text{(Eqs. 15a, b)}$$

Additionally, the measurement update equations are

$$\begin{aligned}\mathbf{K}_k &= \mathbf{P}_k^-\mathbf{C}^T\left(\mathbf{C}\mathbf{P}_k^-\mathbf{C}^T + \sigma_n^2\right)^{-1},\\ \hat{\mathbf{x}}_k &= \hat{\mathbf{x}}_k^- + \mathbf{K}_k\left(\mathbf{y}_k - \mathbf{C}\hat{\mathbf{x}}_k^-\right),\\ \mathbf{P}_k &= \left(\mathbf{I} - \mathbf{K}_k\mathbf{C}\right)\mathbf{P}_k^-.\end{aligned} \qquad \text{(Eqs. 16a, b, c)}$$

where **K** is Kalman gain and **I** is identity matrix.

[0076] **Extended Kalman Filter**

[0077] According to certain embodiments, the Kalman filter 246b may be an extended Kalman filter that is used to estimate the states of nonlinear dynamic system. For nonlinear discrete time system in which the state is a weight (**w**) that is known, the nonlinear version of the dynamic system can be defined as

$$\begin{aligned}\mathbf{x}_k &= \mathbf{F}\left(\mathbf{x}_{k-1}, \mathbf{w}, \mathbf{u}_{k-1}\right) + \mathbf{B}_v\mathbf{v}_k,\\ \mathbf{y}_k &= \mathbf{H}\left(\mathbf{x}_k, \mathbf{w}\right),\end{aligned} \qquad \text{(Eqs. 17a, b)}$$

where **F** is system dynamics, **B** is disturbance injection, **u** is inputs, and **H** is the discrete version for nonlinear measurement function. Additionally, the linearization may be defined at each instant or at intervals, such as, for example, 0.01 second or 1 second

$$\mathbf{A}_k \equiv \left.\frac{\partial \mathbf{F}(\mathbf{x},\mathbf{w},\mathbf{u})}{\partial \mathbf{x}}\right|_{\mathbf{x}=\hat{\mathbf{x}}_k,\mathbf{u}=\mathbf{u}_k}, \mathbf{B}_k \equiv \left.\frac{\partial \mathbf{F}(\mathbf{x},\mathbf{w},\mathbf{u})}{\partial \mathbf{u}}\right|_{\mathbf{x}=\hat{\mathbf{x}}_k,\mathbf{u}=\mathbf{u}_k} \quad \text{(Eqs. 18a, b, c)}$$
$$\mathbf{C}_k \equiv \left.\frac{\partial \mathbf{H}(\mathbf{x}_k,\mathbf{w})}{\partial \mathbf{x}}\right|_{\mathbf{x}=\hat{\mathbf{x}}_k}.$$

[0078] A nonlinear extended Kalman filter may begin with the same initialization as the linear Kalman Filter, as referenced above in Eqs. 18a-c. For $k \in \{1,\cdots,\infty\}$, the time update equations of the extended Kalman filter are

$$\begin{aligned}\hat{\mathbf{x}}_k^- &= \mathbf{F}(\mathbf{x}_{k-1},\mathbf{w},\mathbf{u}_{k-1}),\\ \mathbf{P}_k^- &= \mathbf{A}_{k-1}\mathbf{P}_{k-1}\mathbf{A}_{k-1}^T + \mathbf{B}_v\sigma_v^2\mathbf{B}_v.\end{aligned} \quad \text{(Eqs. 19a, b)}$$

with σ being the covariance of noise, and the measurement update equations, which may be used by the vehicle parameter estimation of Figure 3, being

$$\begin{aligned}\mathbf{K}_k &= \mathbf{P}_k^-\mathbf{C}_k^T\left(\mathbf{C}_k\mathbf{P}_k^-\mathbf{C}_k^T + \sigma_n^2\right)^{-1}\\ \hat{\mathbf{x}}_k &= \hat{\mathbf{x}}_k^- + \mathbf{K}_k\left(\mathbf{y}_k - \mathbf{H}\left(\hat{\mathbf{x}}_k^-,\mathbf{w}\right)\right)\\ \mathbf{P}_k &= \left(\mathbf{I} - \mathbf{K}_k\mathbf{C}_k\right)\mathbf{P}_k^-.\end{aligned} \quad \text{(Eqs. 20a, b, c)}$$

[0079] **Extended Kalman Weight Filter**

[0080] According to embodiments in which the Kalman filter 246b is being used to estimate the weight of the vehicle, the Kalman filter 246 may be an extended Kalman weight filter that is used to estimate the weights of a nonlinear dynamic system. The recursive weight estimation for the weight (**w**) of the vehicle 200 can be developed by giving the weights their own state-space representation:

$$\begin{aligned}\mathbf{w}_k &= \mathbf{w}_{k-1}\\ \mathbf{x}_k &= \mathbf{F}(\mathbf{x}_{k-1},\mathbf{w}_k) + \mathbf{n}_k\end{aligned} \quad \text{(Eqs. 21a, b)}$$

Where **F** is the system dynamics, and **n** is disturbance.

[0081] The extended Kalman weight filter equations may start with initializing

$$\hat{\mathbf{w}}_0 = E[\mathbf{w}]$$
$$\mathbf{Q}_0 = E\left[(\mathbf{w} - \hat{\mathbf{w}}_0)(\mathbf{w} - \hat{\mathbf{w}}_0)^T\right] \quad \text{(Eqs. 22a, b)}$$

where E is expectation, $\mathbf{Q}$ is estimation error covariance, and T is matrix transform.

[0082] For $k \in \{1, \cdots, \infty\}$, the time update equation of the Kalman Filter are

$$\hat{\mathbf{w}}_k = \hat{\mathbf{w}}_{k-1},$$
$$\mathbf{Q}_k^- = \lambda^{-1}\mathbf{Q}_k^-, \quad \text{(Eqs. 23a, b)}$$

where λ is a forgetting factor that gives exponentially less weight to older error samples or measurements. The measurement update equations, which may be used by the vehicle parameter estimation of Figure 3 are

$$\mathbf{K}_k^w = \mathbf{Q}_k^- \mathbf{H}_k^T \left(\mathbf{H}_k^T \mathbf{Q}_k^- \mathbf{H}_k^T + \sigma_n^2\right)^{-1}$$
$$\hat{\mathbf{w}}_k = \hat{\mathbf{w}}_k^- + \mathbf{K}_k^w \left(\mathbf{x}_k - \mathbf{F}\left(\mathbf{x}_{k-1}, \mathbf{w}_k\right)\right) \quad \text{(Eqs. 24a, b, c)}$$
$$\mathbf{Q}_k = \left(\mathbf{I} - \mathbf{K}_k^w \mathbf{H}_k\right)\mathbf{Q}_k^-$$

[0083] **Dual Estimation**

[0084] According to certain embodiments, the Kalman filter 246a, 246b uses dual estimation is the combination of states estimation and weights estimation. More specifically, when available signals are noisy, such as, for example, numerous signals being provided to the control block 110 from a sensor 108, as well as the variances in those signals, it may be problematic and/or impossible to determine system weights identification merely by only estimating the model. Thus, dual estimation may be required to obtain accurate system weights.

[0085] **Dual Estimation Using Dual Extended Kalman Filter**

[0086] Figure 5 illustrates a block diagram of a Kalman filter 246b that includes an extended Kalman state filter 120 and an extended Kalman weight filter 122. According to certain embodiments, however, the extended Kalman state filter 120 and the extended Kalman weight filter 122 may be unscented Kalman filters. The extended Kalman state filter 120 and extended Kalman weight filter 122 may be operated

concurrently and involve recursive derivative calculation. Such concurrent operation may allow for the Kalman filter 246 to provide dual estimation for the combination of states and weight estimations. More specifically, the extended Kalman state filter 120 generates states estimates ($\hat{\mathbf{x}}_k$) and requires $\hat{\mathbf{w}}_{k-1}$ (posterior weight estimation) for the time update. The extended Kalman weight filter 122 generates weight estimation ($\hat{\mathbf{w}}_k$) and requires $\hat{\mathbf{x}}_{k-1}$ for the measurement update.

[0087] As shown a measurement (y_k) is provided to measurement update blocks 124a, 124b for the respective extended Kalman state filter 120 and extended Kalman weight filter 122. The measurement update blocks 124a, 124b then use the provided measurement (y_k) as well as with the priori estimation provided from a time update block 126a, 126b, such as $\hat{\mathbf{x}}_k^-$ or $\hat{\mathbf{w}}_k^-$, as shown in Figure 5. The resulting estimate ($\hat{\mathbf{x}}_k$ or $\hat{\mathbf{w}}_k$) may then be provided for use by the control block 110 for the associated vehicle control system. Additionally, the resulting estimate from the measurement update blocks 124a, 124b are also feed back to the associated time update block 126a, 126b as $\hat{\mathbf{w}}_{k-1}$ or $\hat{\mathbf{x}}_{k-1}$ for subsequent use by the time update block 126a, 126b in generating another priori estimation. As shown, the time update block 126a is illustrated as having multiple arrows, indicating the system as having dynamics, while the parameters associated with time update block 126b is assumed to have no dynamics.

[0088] **Dual Estimation Joint Extended Kalman Filter**

[0089] Alternatively, according to certain embodiments, the Kalman filter 246b may act as a joint extended Kalman filter that generates dual estimation by treating the weights ($\mathbf{w}$) the same way as the states ($\mathbf{x}$) are treated, and by extending the system states as follows

$$\mathbf{z}_k = \begin{bmatrix} \mathbf{x}_k \\ \mathbf{w}_k \end{bmatrix} \qquad \text{(Eq. 25)}$$

The extended nonlinear discrete time system may then be rewritten in

$$\begin{bmatrix} \mathbf{x}_k \\ \mathbf{w}_k \end{bmatrix} = \begin{bmatrix} \mathbf{F}(\mathbf{z}_{k-1}, \mathbf{u}_{k-1}) \\ 0 \end{bmatrix} + \begin{bmatrix} 0 & 0 \\ 0 & \mathbf{I} \end{bmatrix} \mathbf{z}_k + \begin{bmatrix} \mathbf{B}_v \mathbf{v}_k \\ 0 \end{bmatrix} \qquad \text{(Eq. 26)}$$
$$\mathbf{y}_k = \mathbf{H}(\mathbf{z}_k),$$

Further, if one were to consider that

$$\mathbf{F}'(\mathbf{z}_{k-1},\mathbf{u}_{k-1}) = \begin{bmatrix} \mathbf{F}(\mathbf{z}_{k-1},\mathbf{u}_{k-1}) \\ 0 \end{bmatrix} + \begin{bmatrix} 0 & 0 \\ 0 & \mathbf{I} \end{bmatrix} \mathbf{z}_k \qquad \text{(Eq. 27)}$$

then the dual estimation problem becomes the same as the standard extended Kalman filter. More specifically, when viewing the augmented vector $[\mathbf{x}_k\ \mathbf{w}_k]$ as x_k, they are the same problem in that there is no difference in implementing a non-joint and a joint version Kalman filter when augmentation is ignored.

[0090] Dual Estimation With Colored Noise

[0091] When measurement noise is colored noise, the noise can be thought of as an additional signal. Colored noise may be is modeled as an auto-regression model that is driven by some other white noise signal. When white noise passes through an auto-regressive structure, the color of the white noise may be changed accordingly. Thus, the extended part of the state space is

$$\mathbf{n}_k = \mathbf{A}_n \mathbf{n}_{k-1} + \mathbf{B}_n \mathbf{v}_{n,k}.$$

$$A_n = \begin{bmatrix} w_n^{(1)} & w_n^{(2)} & \cdots & w_n^{(M_n)} \\ 1 & 0 & 0 & 0 \\ 0 & \ddots & 0 & \vdots \\ 0 & 0 & 1 & 0 \end{bmatrix} \qquad \text{(Eq. 28)}$$

where **n** is noise, and the subscript n is the weight (parameter) for the autoregressive structure which is related to the characteristics of the noise.

[0092] For embodiments in which the Kalman filter 246b is a dual extended Kalman filter estimation, the extended states are

$$\xi_k = \begin{bmatrix} \mathbf{x}_k \\ \mathbf{n}_k \end{bmatrix}, \qquad \text{(Eq. 29)}$$

where ξ is a states vector that is augmented with parameter of the autoregressive model for noise. With the joint extended Kalman filter, the extended states, which may be a compilation of the real system states, system unknown parameters, and noise structure parameters, are

$$\xi_k = \begin{bmatrix} \mathbf{z}_k \\ \mathbf{n}_k \end{bmatrix}. \qquad \text{(Eq. 30)}$$

[0093] **A. Unscented Kalman Filter**

[0094] According to certain embodiments, the Kalman filter 246b may be an unscented Kalman filter. The basic steps of an unscented Kalman filter 246b can be described as follows. The steps may initialize with

[0095] $$\hat{\mathbf{x}}_0 = \mathbf{E}(\mathbf{x}_0),\ P_0 = \mathbf{E}\left((\mathbf{x}_0 - \hat{\mathbf{x}}_0)(\mathbf{x}_0 - \hat{\mathbf{x}}_0)^T\right) \qquad \text{(Eqs. 31a, b)}$$

[0096] where P is error covariance, **E** is expectation, and T is transpose.

[0097] Further, for $k \in \{1, \cdots, \infty\}$, calculating the sigma points

$$\chi_{k-1} = \left[\hat{\mathbf{x}}_{k-1} \quad \hat{\mathbf{x}}_{k-1} + \gamma\sqrt{\mathbf{P}_{k-1}} \quad \hat{\mathbf{x}}_{k-1} - \gamma\sqrt{\mathbf{P}_{k-1}}\right]. \qquad \text{(Eq. 32)}$$

where **P** is the estimation covariance and γ is a scaling factor. The time-update equations for the states are

$$\begin{aligned} \chi^*_{k|k-1} &= \mathbf{F}(\chi_{k-1}, \mathbf{u}_{k-1}), \\ \hat{\mathbf{x}}^-_k &= \sum_{i=0}^{2L} \mathbf{W}_i^{(m)} \chi^*_{i,k|k-1}, \\ \mathbf{P}^-_k &= \sum_{i=0}^{2L} \mathbf{W}_i^{(c)} \left(\chi^*_{i,k|k-1} - \hat{\mathbf{x}}^-_k\right)\left(\chi^*_{i,k|k-1} - \hat{\mathbf{x}}^-_k\right)^{\mathrm{T}} + \mathbf{Q}, \\ \chi_{k|k-1} &= \left[\hat{\mathbf{x}}^-_k \quad \hat{\mathbf{x}}^-_k + \gamma\sqrt{\mathbf{P}^-_k} \quad \hat{\mathbf{x}}^-_k - \gamma\sqrt{\mathbf{P}^-_k}\right]. \end{aligned} \qquad \text{(Eq. 33a-d)}$$

The time update equations for the priori estimation of measurements are

$$\begin{aligned} \mathscr{Y}_{k-k-1} &= H\left[\chi_{k|k-1}\right] \\ \hat{\mathbf{y}}^-_k &= \sum_{i=0}^{2L} \mathbf{W}_i^{(m)} \mathscr{Y}^*_{i,k|k-1}, \\ \mathbf{P}^-_{yy} &= \sum_{i=0}^{2L} \mathbf{W}_i^{(c)} \left(\mathscr{Y}_{i,k|k-1} - \hat{\mathbf{y}}^-_k\right)\left(\mathscr{Y}_{i,k|k-1} - \hat{\mathbf{y}}^-_k\right)^{\mathrm{T}} + \mathbf{R}, \end{aligned} \qquad \text{(Eq. 34a-c)}$$

The posterior measurement update equations are

$$\mathbf{P}_{xy} = \sum_{i=0}^{2L} \mathbf{W}_i^{(c)} \left(\boldsymbol{\chi}^{*}_{i,k|k-1} - \hat{\mathbf{x}}_k^- \right) \left(\mathcal{Y}_{i,k|k-1} - \hat{\mathbf{y}}_k^- \right)^T,$$
$$\mathbf{K}_k = \mathbf{P}_{xy} \mathbf{P}_{yy}^{-1}, \qquad \text{(Eq. 35a-d)}$$
$$\hat{\mathbf{x}}_k = \hat{\mathbf{x}}_k^- + \mathbf{K}_k \left(\mathbf{y}_k - \hat{\mathbf{y}}_k \right),$$
$$\mathbf{P}_k = \mathbf{P}_k^- - \mathbf{K}_k \mathbf{P}_{yy} \mathbf{K}_k^T.$$

The weights (**W**) for Eq. 35 are calculated using

$$\mathbf{W}_0^{(m)} = \lambda / \left(L + \lambda \right),$$
$$\mathbf{W}_0^{(c)} = \lambda / \left(L + \lambda \right) + \left(1 - \alpha^2 + \beta \right), \qquad \text{(Eq. 36a-c)}$$
$$\mathbf{W}_i^{(m)} = \mathbf{W}_i^{(c)} = 1 / \left(2 \left(1 + \lambda \right) \right) \quad i = 1, \ldots, 2L,$$

where the composite scaling factor is

$$\lambda = \alpha^2 \left(L + k \right) - L \qquad \text{(Eq. 37)}$$

where α is the scaling factor that determines the spread of the sigma points; k designates the scaling direction of sigma points; and, β incorporates high order effects by adding the weighting of zero sigma point of the calculation of covariance. Additional complexity is added to the algorithm by using covariance matching to adaptively select measurement noise covariance matrix **R**.

[0098] **B. Road Curvature Representation**

[0099] Figure 17 illustrates a vehicle 200 travelling in the vertical plane at three different locations (a), (b), (c) along a road 114. As shown, each of the three locations have different elevations or grades. More specifically, at location (a), the vehicle 200 is traveling along a portion of the road 114 that has a relatively steep grade. Conversely, when at location (b), the vehicle 200 is traveling along a relatively flat portion of the road 114, with little, if any, incline. At location (c), the vehicle 200 is traveling along a location of the road that has a grade that is greater than road 114 has at location (b) but less than the grade of the road 114 at location (a).

[00100] As the vehicle travels along the road 114, variances in the grade of the road 114, as well as other environmental and operational conditions, may cause variances in vehicle parameters, such as, for example, rolling resistance, aerodynamic drag

coefficient, and vehicle weight. Knowledge of such vehicle parameters however may be used to improve the accuracy of longitudinal vehicle control system 100, and more specifically the models on which such control systems are based, including for example, determining optimal setting for cruise control and/or gear settings for the transmission of the vehicle, among others. However, constant variances in such parameters may result in measurement noise that may need to be resolved in order to derive the particular information that will allow for an accurate model to be developed for the longitudinal vehicle control system 100. To attain such accuracy, certain embodiments of the present technology employ dual estimation of vehicle parameters using a Kalman Filter 246, such as an extended or unscented Kalman filter. Further, dual estimation may be the combination of states and parameters.

[00101] Referencing Figure 17, the road profile elevation (E), such as reference zero elevation at the current altitude, and may be expressed as a function of distance, such as $E = E(s)$. The road profile elevation may assist in deriving certain operational parameters of the vehicle 200, such as, for example, the road profile curvature (κ). The road profile curvature may then be used to derive other operational parameters, such as, for example, the force exerted in an X axis on or by the vehicle 200, as discussed below. For example, road profile elevation (E) may be used for calculating the road profile curvature (κ) as follows

$$\kappa = \frac{E}{\left(1+E'^2\right)^{3/2}} \qquad \text{(Eq. 38)}$$

where E' is the derivative of road profile elevation with respect to distance.

[00102] Changing the derivative E' with respect to time yields

$$E' = \frac{dE}{ds} = \frac{dE}{dt}\frac{dt}{ds} = \frac{dE}{dt}\frac{1}{v} \qquad \text{(Eq. 39a)}$$

$$E'' = \frac{d\mathrm{E}'}{ds} = \frac{d}{ds}\left(\frac{dE}{dt}\frac{1}{v}\right) = \frac{d}{dt}\left(\frac{dE}{dt}\frac{1}{v}\right)\frac{dt}{ds} \qquad \text{(Eq. 39b)}$$

$$= \left(\frac{d^2E}{dt^2} \frac{1}{v} - \frac{dE}{dt} \frac{\dot{v}}{v^2} \right) \frac{1}{v} = \frac{d^2E}{dt^2} \frac{1}{v^2} - \frac{dE}{dt} \frac{\dot{v}}{v^3}$$

with v representing the parameter of vehicle speed.

[00103] Substituting Eqs. 39a and 39b into Eq. 38 allows the road profile curvature (κ) to be expressed as

$$\kappa = \frac{\frac{d^2E}{dt^2} \frac{1}{v^2} - \frac{dE}{dt} \frac{\dot{v}}{v^3}}{\left(1 + \left(\frac{dE}{dt} \frac{1}{v} \right)^2 \right)^{3/2}} = \frac{\frac{1}{v^2} - \dot{E} \frac{\dot{v}}{v^3}}{\left(1 + \left(\frac{\dot{E}}{v} \right)^2 \right)^{3/2}} \qquad \text{(Eq. 40)}$$

[00104] Additionally, a change in vehicle elevation and the speed the vehicle 200 is travelling along the road 114 may be constrained by the road gradient (ϕ). Therefore, the road profile elevation (E) may also be expressed as follows

$$E = v \sin(\phi) \qquad \text{(Eq. 41)}$$

[00105] Eq. 41 may be substituted into Eq. 40, thereby allowing the road profile curvature (κ) to be expressed as

$$\kappa = \frac{1}{v^2} \frac{v \cos(\phi) \dot{\phi}}{\left(1 + \sin(\phi)^2 \right)^{3/2}} = \frac{\cos(\phi) \phi}{v \left(1 + \sin(\phi)^2 \right)^{3/2}} \qquad \text{(Eq. 42)}$$

[00106] **B. Vehicle Longitudinal and Pitch Dynamics**

[00107] Figure 18 illustrates the planner dynamics of a vehicle 200 that is on an inclined and curved road 114. As shown, a vector (a) indicates the vehicle 200 is traveling with a speed (v) in a forward direction that is generally in line with the x axis, while the top portion 116 of the vehicle 200 is generally facing the z axis. Additionally, the center of gravity (C) of the vehicle 200 is spaced from the front and rear axles of the vehicle 200 by a distance *a1* and *a2*, respectively. The road 114 has a curvature having radius indicated by R_H. The vehicle 200 also provides a downward force indicated by mg, where m is the mass of the vehicle 200 and g is the gravitational force. Figure 18 also

indicates the road gradient (ϕ) as well as an angle (Θ) of the road curvature. Further, F_{x1} and F_{x2} represent propelling forces, while F_{z1} and F_{z2} represent normal forces.

[00108] Based on Newton's law, the propelling force (F_x), the normal force (F_z), and the force moment (M_y) of the vehicle 200 may be satisfied by the following

$$\sum F_x = m_{eq}\dot{v} \quad \text{(Eq. 43a)}$$

$$\sum F_z = \kappa m v^2 \quad \text{(Eq. 43b)}$$

$$\sum M_y = I_y\ddot{\phi} \quad \text{(Eq. 43c)}$$

where m_{eq} is the equivalent mass and I_y is the moment of inertia about the y axis.

[00109] Assuming the secant and tangent of the road 114 curvature are relatively accurate, the motion of the vehicle 200 may be expressed as

$$m_{eq}\dot{v} = F_{x1} + F_{x2} - mg\sin(\phi) - (F_{z1} + F_{z2})(R_{c0} + R_{c1}v)\left(\frac{2}{1+\exp(-40v)} - 1\right) - \frac{1}{2}\rho C_d v^2 \quad \text{(Eq. 44a)}$$

$$\kappa m v^2 = F_{z1} + F_{z2} - mg\cos(\phi) \quad \text{(Eq. 44b)}$$

$$I_y\ddot{\phi} = F_{z1}a_1 - F_{z2}a_2 + (F_{x1} + F_{x2})h \quad \text{(Eq. 44c)}$$

where R_{c0} is rolling resistance zero order, R_{c1} is rolling resistance first order, ρ is air density, C_d is the coefficient of drag, and h is the center of height of gravity.

[00110] In Eq. 44a, the rolling resistance(s) (R_{c0} and R_{c1}) is/are modified by a hyperbolic tangent sigmoid function. Such a modification attempts to avoid a relatively large rolling resistance being derived while the vehicle 200 is not moving but while differential Eq. 44a remains analytic.

[00111] Substituting Eq. 42 into Eq. 44 yields

$$m_{eq}\dot{v} = F_{x1} + F_{x2} - mg\sin(\phi) - (F_{z1} + F_{z2})(R_{c0} + R_{c1}v)\left(\frac{2}{1+\exp(-40v)} - 1\right) - \frac{1}{2}\rho C_d v^2 \quad \text{(Eq. 45a)}$$

$$\frac{mv\cos(\phi)\dot{\phi}}{\left(1+\sin(\phi)^2\right)^{3/2}} = F_{z1} + F_{z2} - mg\cos(\phi)$$

$$I_y\ddot{\phi} = F_{z1}a_1 - F_{z2}a_2 + (F_{x1} + F_{x2})h \quad \text{(Eq. 45b)}$$

[00112] Under the assumption that the propelling forces F_{x1} and F_{x2} of the vehicle 200 can be lumped into one propelling force (F_x), Eqs. 45a and 45b can be rewritten as

$$m_{eq}\dot{v} = F_x - mg\sin(\phi) - (F_{z1} + F_{z2})(R_{c0} + R_{c1}v)\left(\frac{2}{1+\exp(-40v)} - 1\right) - \frac{1}{2}\rho C_d v^2 \quad \text{(Eq. 46a)}$$

$$\frac{mv\cos(\phi)\dot{\phi}}{\left(1+\sin(\phi)^2\right)^{3/2}} = F_{z1} + F_{z2} - mg\cos(\phi) \quad \text{(Eq. 46b)}$$

$$I_y\ddot{\phi} = F_{z1}a_1 - F_{z2}a_2 + F_x h$$

[00113] Eliminating F_{z2} from Eqs. 46a and 46b yields an equation that may be expressed as

$$m_{eq}\dot{v} = F_x - mg\sin(\phi) - m\cos(\phi)\left(\frac{v\dot{\phi}}{\left(1+\sin(\phi)^2\right)^{3/2}} + g\right)(R_{c0} + R_{c1}v)\left(\frac{2}{1+\exp(-40v)} - 1\right) - \frac{1}{2}\rho C_d A v^2 \quad \text{(Eq. 47a)}$$

$$I_y\ddot{\phi} = F_{z1}l - m\cos(\phi)\left(\frac{v\dot{\phi}}{\left(1+\sin(\phi)^2\right)^{3/2}} + g\right)a_2 + F_x h \quad \text{(Eq. 47b)}$$

where A is the frontal area of the vehicle 200 and l is the wheel base distance (sum of a1+a2 from Figure 18). Further, equivalent mass (m_{eg}) and propelling force (F_x) can be represented as

$$m_{eq} = \frac{(J_1 i_1^2 + J_2)i_2^2 + J_3}{R^2} + m \quad \text{(Eq. 48a)}$$

$$F_x = \frac{T i_1 i_2 \eta - T_b}{R} \quad \text{(Eq. 48b)}$$

where J_1 represents engine inertia, J_2 is transmission inertia, J_3 is the inertia of the rotating tire(s), i_1 is the gear ratio, i_2 is the final drive ratio, η is the driveline efficiency, R indicates the radius of the wheel 118 of the vehicle 200, T is the torque of the engine of the vehicle 200, and T_b is brake torque.

[00114] Eq. 47a describes longitudinal vehicle dynamics on an undulated road 114. As shown Eq. 47a contains an extra road gradient time derivative term ($\dot{\phi}$), which is caused by road curvature in the normal force term, or as the vehicle 200 is traveling down the road. More specifically, when the road gradient is increasing, the normal force, *e.g.*, $F_{z1} + F_{z2}$, will be larger than the road normal force on a constant slope. Such behavior indicates that the vehicle 200 has certain pitch dynamics. Additionally, the additional road gradient time derivative term ($\dot{\phi}$) allows for the system of Eq. 47a to extend beyond conventional first order systems having only one measurement and wherein the maximum number of parameters that can be identified is one. Thus, by adding an additional road gradient time derivative term ($\dot{\phi}$), the accuracy normal force for the system of Eq. 47a may be improved.

[00115] Additionally, Eq. 47a is independent of the distribution of normal forces F_{z1} and F_{z2}, as the equation is not impacted by the total normal force. This feature also makes Eq. 47a universal in describing the longitudinal dynamics of a multi-axle vehicle. However, Eq. 47b is not in its closed form because in order to know the dynamic distribution of normal force, the suspension dynamics is required.

[00116] **C. State Space Analysis / State Space Representation**

[00117] According to certain embodiments, the following state space configuration may be assumed

$$\mathbf{x} = \begin{bmatrix} x_1 & x_2 \end{bmatrix}^T = \begin{bmatrix} v & \phi \end{bmatrix}^T \qquad \text{(Eq. 49a)}$$

$$\mathbf{u} = \begin{bmatrix} u_1 & u_2 & u_3 & u_4 \end{bmatrix}^T \qquad \text{(Eq. 49b)}$$

where **x** is a vector having the elements of vehicle velocity and road gradient, **u** is an input to the system, u_1 is engine torque, u_2 is transmission gear ratio, u_3 is brake torque, and u_4 is gradient changing rate as the augmented input.

[00118] Under such assumptions, the longitudinal vehicle dynamics described above by Eq. 47a may be represented as a vehicle system as

$$\dot{x}_1 = \frac{\frac{u_1 u_2 i_2 \eta - u_3}{R} - mg\sin(x_2) - \frac{1}{2}\rho C_d A x_1^2 - m\cos(x_2)\left(\frac{x_1 u_4}{\left(1+\sin(x_2)^2\right)^{3/2}} + g\right)\left(R_{c0} + R_{c1}x_1\right)\left(\frac{2}{1+\exp(-40x_1)} - 1\right)}{\frac{\left(J_1 u_2^2 + J_2\right) i_2^2 + J_3}{R^2} + m} \quad \text{(Eq. 50a)}$$

$$\dot{x}_2 = u_4 \quad \text{(Eq. 50b)}$$

with the measurement of vehicle speed being $\mathbf{y} = x_1$. Observable parameters are

$$\mathbf{w} = \begin{bmatrix} m \\ u_4 \end{bmatrix} \quad \text{(Eq. 51)}$$

[00119] **D. Observability and Identifiability**

[00120] Eqs. 40a and 40b and their measurements in vector form can be rewritten in the general nonlinear system equations

$$\dot{\mathbf{x}} = \mathbf{f}(\mathbf{x}, \mathbf{u}), \quad \mathbf{y} = \mathbf{h}(\mathbf{x}) \quad \text{(Eq. 52)}$$

[00121] The observability of the nonlinear system described by Eq. 52 is determined by the rank of the following observability matrix

$$O = \begin{bmatrix} \nabla L_{\mathbf{f}}^0 h_1 \\ \cdots \\ \nabla L_{\mathbf{f}}^0 h_r \\ \cdots \\ \nabla L_{\mathbf{f}}^{n-1} h_1 \\ \cdots \\ \nabla L_{\mathbf{f}}^{n-1} h_r \end{bmatrix} \quad \text{(Eq. 53)}$$

Where n is the dimension of the state space, ∇ denotes gradient, and the Lie Derivative $L_{\mathbf{f}}^{n-1}h_i$ is defined as the derivative of a scalar function along a vector field

$$\begin{aligned} L_{\mathbf{f}}^{0}h &= h, \\ L_{\mathbf{f}}^{1}h &= \nabla h \cdot \mathbf{f}, \\ L_{\mathbf{f}}^{2}h &= \nabla\left(L_{\mathbf{f}}^{1}h\right)\cdot \mathbf{f} \\ &\cdots \\ L_{\mathbf{f}}^{n-1}h &= \nabla\left(L_{\mathbf{f}}^{n-2}h\right)\cdot \mathbf{f} \end{aligned} \qquad \text{(Eq. 54)}$$

[00122] Considering that the observability matrix O will be dependent on states and input, the inferred observability will be only local. If the rank of matrix O equals n then the system is locally observable, otherwise the system is not locally observable. Moreover, observability indicating an incomplete measurement set, which may be a function of partially states and input, may address whether the whole states which can uniquely define the system's behavior can be known. However, if the rank of matrix O is independent of the states and the inputs, then the system is locally observable everywhere, and thus globally observable.

[00123] Identifiability is defined as the observability of the parameters, such as, for example, vehicle mass, rolling resistance, and/or the coefficient of drag, among others. Assuming unknown parameters, as denoted by **w**, are time invariant or at least slowly time varying, then

$$\dot{\mathbf{x}} = \mathbf{f}\left(\mathbf{x},\mathbf{u},\mathbf{w}\right) \qquad \text{(Eq. 55a)}$$

$$\dot{\mathbf{w}} = 0 \qquad \text{(Eq. 55b)}$$

$$\mathbf{y} = \mathbf{h}\left(\mathbf{x},\mathbf{w}\right) \qquad \text{(Eq. 55c)}$$

with **x** being the states.

[00124] The corresponding parameter identifiability may then be determined by the rank of matrix

$$O_{\mathbf{w}} = \begin{bmatrix} \nabla_{\mathbf{w}} L_{\mathbf{f}}^{0} h_1 \\ \cdots \\ \nabla_{\mathbf{w}} L_{\mathbf{f}}^{0} h_r \\ \cdots \\ \nabla_{\mathbf{w}} L_{\mathbf{f}}^{n-1} h_1 \\ \cdots \\ \nabla_{\mathbf{w}} L_{\mathbf{f}}^{n-1} h_r \end{bmatrix} \qquad \text{(Eq. 56)}$$

where $\nabla_{\mathbf{w}}$ denotes the gradient of a scalar in a Cartesian vector space defined by Eq. 49a, 49b with respect to the unknown parameter vector w.

[00125] Applying the observability and identifiability checks of Eqs. 53 and 56 on the longitudinal vehicle dynamics system 100 of Eq. 40a yields several conclusions. First, the system of Eq. 40a is full state observable with vehicle speed measurement, and thus, from one measurement, all other states are known. Second, the maximum number of identifiable parameters is two. Further, of those two parameters, one is to be the road grade changing rate so as to make road grade an observable state. These conclusions indicate that in order to reconstruct the unknown road grade information, which is an input to the system at Eq. 40a, there is only one extra parameter that is to be identified. It is possible to increase the number of parameters that can be identified, such as, for example, by considering suspension dynamics and associated dynamic distribution of normal force. However, according to certain embodiments, such additional structure may be problematic, as such additional structure, which result in additional parameters, may cause problems that will increase the difficulty in implementation. For example, additional parameters could dramatically increase computational intensity, which may increase computational time and thereby delay the response time for providing accurate system information. Additionally, such an increase in computational intensity may also place greater demands on the associated control units or modules that are making such computations, thereby requiring more, or larger, hardware that can adequately, and timely, handle the associated demand, as well as continue to provide other vehicle and/or engine functional requirements, if any. Further, the introduction of additional parameters may include parameters having uncertain or estimated, but not measured, values, which may or may not adversely impact the accuracy of the system.

[00126] **E. Simulation**

[00127] Figures 19 and 20 illustrate simulations of road grade and vehicle mass, respectively, in which the Kalman filter 246b is an unscented Kalman filter, and in which the perfect noise free measurement is assumed. Figure 19 illustrates set changes in road elevation, with the variations in the simulated road grade having a sinusoidal shape. In the table to the left, the initial guess as to the road grade is approximately 4, while the chart on the right in Figure 19 illustrates an initial guess that the road grade is approximately -3.6. Further, in the chart on the left in Figure 20, the initial guess of the weight of the vehicle 200 starts at 50% lower than the actual set weight, while the chart to the right has the initial weight at 150%, or 50% above the actual set weight. As shown, within 100 seconds, the estimated vehicle mass in Figure 20 is within 2% error bound from the real value. After 100 seconds, the estimated road grade is also tracking the real road grade change very well. Figures 19 and 20 illustrate that it is possible to estimate vehicle mass and road grade without the measurement of road elevation. Further, as shown, these simulations illustrate that no matter what is the original guess, the degeneration mode algorithm, *e.g.*, Eqs. 33-37 wherein the **F** in Eq. 21a will be replaced with the discrete version of Eqs. 55a and 55b, will give very similar results for road grade.

[00128] Assuming the measurement of vehicle speed is corrupted by noise with a standard deviation of 0.1m/s (covariance 0.01), an estimation algorithm with parameter estimation algorithm only may not converge to a desired error bound. In such situations, a states and parameter estimation may need to be done simultaneously. While the simulations shown in Figures 19 and 20 involved an unscented Kalman filter, similar simulations may also be done using an adaptive joint unscented Kalman filter algorithm. Moreover, an adaptive unscented Kalman filter algorithm with covariance matching may estimate the nominal covariance of the real measurement noise.

[00129] **II. Normal Mode Joint Unscented Kalman Filter**

[00130] When the vehicle positioning and horizon generation system 214 is functional, *e.g.,* when the map data is available, a Kalman filter 246a. such as, for example a joint or dual unscented or extended Kalman filter, may be in the normal mode.

Accordingly, the control inputs may be provided to the Kalman filter 246a from the nonlinear adaptive cruise controller 232, while the states may be provided by a states vector. Thus, the road profile, and more specifically the profile of the road in the horizon, may be provided to the normal mode Kalman filter 246a from the vehicle positioning and horizon generation system 214. The Kalman filter 246a may then be used to estimate, with the assistance of information from the vehicle positioning and horizon generation system 214, vehicle mass, aerodynamic drag, and rolling resistance.

A. State Space Analysis: State Space Representation

[00131] Transient engine torque can be represented by

$$\dot{T}_e = -\frac{1}{\tau}T_e + \frac{1}{\tau}T_{ecmd}. \qquad \text{(Eq. 57)}$$

[00132] Augmenting the system in in which the vehicle distance D_{ist} and the vehicle elevation E, assuming the following state space configuration

$$\mathbf{x} = \begin{bmatrix} x_1 & x_2 & x_3 & x_4 & x_5 \end{bmatrix}^T = \begin{bmatrix} v & \phi & D_{ist} & E & T_e \end{bmatrix}^T$$
$$\mathbf{u} = \begin{bmatrix} u_1 & u_2 & u_3 & u_4 \end{bmatrix}^T = \begin{bmatrix} u & i_1 & T_b & \dot{\phi} \end{bmatrix}^T \qquad \text{(Eq. 58)}$$

[00133] The longitudinal and vertical vehicle dynamics combined with transient engine torque model can be represented as the fifth order system

(Eq. 59)

where T_{max} and T_{min} are the maximum and minimum torque curves, respectively, and u_1 is the throttle command.

[00134] Assuming all states on the vehicle level are measurable, the measurements are $y = [x_1\ x_2\ x_3\ x_4]^T$, the observable parameters are

$$\mathbf{w} = \begin{bmatrix} m \\ C_d \\ R_{e0} \end{bmatrix} \qquad \text{(Eq. 60)}$$

[00135] ### C. Simulation

[00136] Figure 16 illustrates data from two simulation tests of the normal mode unscented Kalman filter. In conducting this testing, a perfect noise free measurement is

assumed. The parameters to be estimated in Figure 16, namely vehicle mass, aerodynamic drag, and rolling resistance all start from 50% of the actual values. As shown, it is possible to estimate vehicle mass, aerodynamic drag and rolling resistance simultaneously. After approximately 100 seconds, all three parameters converge close to the real values. The convergences of all three parameters are different mainly because the parameter values are of different magnitude. For example, vehicle mass is easier to converge to the real value than rolling resistance because the value for vehicle mass is much larger than rolling resistance. This makes the error of vehicle mass the largest portion of the total error.

[00137] III. Nonlinear Controller Design for Vehicle Traveling on Undulated Road

[00138] According to certain embodiments, the nonlinear adaptive cruise controller 232 includes a plurality of nonlinear states transformation blocks 234, 236. According to certain embodiments, the plurality of nonlinear states transformation blocks 234, 236 are two identical nonlinear states transformation blocks. Further, a first nonlinear states transformation block 234 may be utilized for a desired trajectory of the state space, which may include the vehicle speed, and receives information regarding desired parameters and information, such as, for example, desired vehicle speed, among other inputs. Further, the second nonlinear states transformation block 236 is utilized for a desired actual trajectory, and receives information regarding actual parameters and information, such as, for example, actual vehicle speed, among other inputs. Estimated vehicle parameters, such as, for example, vehicle mass, aerodynamic drag, and rolling coefficient may be provided to the first and second nonlinear states transformation blocks 234, 236, as well as to a nonlinear inputs transformation block 238. The first and second nonlinear states transformation blocks 234, 236 and the nonlinear inputs transformation block 238 may be implemented to linearize a nonlinear system globally everywhere in the state space.

[00139] A. Definition Relative Degree

[00140] The relative degree of the nonlinear system is the smallest integer $L_g\left(L_f^{r-1}h\right) \neq 0$ and $L_g\left(L_f^{r-2}h\right) = 0 \; \forall \; \mathbf{x}$ in some neighborhood of the defined operation point$\mathbf{x}_0$.

[00141] **B. System with Small Road Curvature Assumption**

[00142] Assuming the road curvature is small and road grade changing rate is small, the simplified state space system can be represented by

$$\begin{aligned}\dot{\mathbf{x}} &= \mathbf{f}(\mathbf{x},d)+\mathbf{g}\begin{bmatrix}u_1\\u_2\\u_3\end{bmatrix}\\ &= \mathbf{f}(\mathbf{x},d)+\mathbf{g}_1u_1+\mathbf{g}_1u_2+\mathbf{g}_1u_3 \qquad \text{(Eq. 61)}\\ \mathbf{y} &= \mathbf{h}(\mathbf{x}) = \begin{bmatrix}1&0&0&0\\0&1&0&0\\0&0&1&0\end{bmatrix}\mathbf{x}\end{aligned}$$

where the process vector field is

$$\mathbf{f}(\mathbf{x},d)=\begin{bmatrix}\dfrac{x_2x_3i_2\eta-x_4}{R}-mg\sin(d)-\dfrac{1}{2}\rho C_dAx_1^2\\ \dfrac{-m\cos(d)\,g\left(R_{c0}+R_{c1}x_1\right)\left(\dfrac{2}{1+\exp(-40x_1)}-1\right)}{\dfrac{\left(J_1x_3^2+J_2\right)i_2^2+J_3}{R^2}+m}\\ 0\\0\\0\end{bmatrix} \qquad \text{(Eq. 62)}$$

the input vector fields is

$$\mathbf{g}_1=\begin{bmatrix}0\\1\\0\\0\end{bmatrix},\ \mathbf{g}_2=\begin{bmatrix}0\\0\\1\\0\end{bmatrix},\ \mathbf{g}_3=\begin{bmatrix}0\\0\\0\\1\end{bmatrix} \qquad \text{(Eq. 63)}$$

[00143] The corresponding decoupling matrix is then changed to

$$\mathbf{A}_{dec}(\mathbf{x})=\begin{bmatrix}L_{\mathbf{g}_1}\left(L_{\mathbf{f}}^1h_1\right) & L_{\mathbf{g}_1}\left(L_{\mathbf{f}}^1h_1\right) & L_{\mathbf{g}_1}\left(L_{\mathbf{f}}^1h_1\right)\\ 1&0&0\\0&1&0\end{bmatrix} \qquad \text{(Eq. 64)}$$

where

$$L_{\mathbf{g}_1}\left(L_{\mathbf{f}}^1 h_1\right)=\frac{x_3 i_2 \eta}{R\left(\frac{\left(J_1 x_3^2+J_2\right) i_2^2+J_3}{R^2}+m\right)},\ L_{\mathbf{g}_3}\left(L_{\mathbf{f}}^1 h_1\right)=\frac{-1}{R\left(\frac{\left(J_1 x_3^2+J_2\right) i_2^2+J_3}{R^2}+m\right)}$$

$$L_{\mathbf{g}_2}\left(L_{\mathbf{f}}^1 h_1\right)=\frac{x_2 i_2 \eta}{R\left(\frac{\left(J_1 x_3^2+J_2\right) i_2^2+J_3}{R^2}+m\right)}$$

$$-\frac{2\left(\begin{array}{l}\frac{x_2 x_3 i_2 \eta-x_4}{R}-mg\sin(d)-\frac{1}{2}\rho C_d A x_1^2 \\ -m\cos(d)\,g\left(R_{c0}+R_{c1}x_1\right)\left(\frac{2}{1+\exp(-40x_1)}-1\right)\end{array}\right) J_1 x_3 i_2^2}{R^2\left(\frac{\left(J_1 x_3^2+J_2\right) i_2^2+J_3}{R^2}+m\right)^2}. \qquad \text{(Eq. 65)}$$

[00144] It is obvious that the non-singularity of the decoupling matrix is ensured. And for the system in Eq. 62 the total relative degree $r=r_1+r_2+r_3=4=n$. Then the nonlinear transformation can be fully defined.

[00145] **C. Controllability**

[00146] **Definition of Lie Bracket:** Considering two vector fields $\mathbf{f}(\mathbf{x})$ and $\mathbf{g}(\mathbf{x})$ in $\mathbb{R}^n$, the Lie bracket operation generates a new vector field

$$[\mathbf{f},\mathbf{g}]=\nabla\mathbf{g}\times\mathbf{f}-\nabla\mathbf{f}\times\mathbf{g}. \qquad \text{(Eq. 66)}$$

[00147] Also high order Lie brackets can be defined:

$$\begin{aligned}&\left(ad_{\mathbf{f}}^1,\mathbf{g}\right)=[\mathbf{f},\mathbf{g}]\\&\left(ad_{\mathbf{f}}^2,\mathbf{g}\right)=\left[\mathbf{f},[\mathbf{f},\mathbf{g}]\right]\\&\cdots\\&\left(ad_{\mathbf{f}}^k,\mathbf{g}\right)=\left[\mathbf{f},\left(ad_{\mathbf{f}}^{k-1},\mathbf{g}\right)\right]\end{aligned} \qquad \text{(Eq. 67)}$$

[00148] **Controllability Theorem** The system defined by:

$$\dot{\mathbf{x}}=\mathbf{f}(\mathbf{x})+\sum_{i=1}^{m}\mathbf{g}_i(\mathbf{x})u_i,\ \ \mathbf{x}\in\mathbb{R}^n \qquad \text{(Eq. 68)}$$

is locally accessible about $\mathbf{x}_0$ if the accessible distribution C spans in the $\mathbb{R}^n$ space. In other words the rank of matrix defined by

$$C=\begin{bmatrix}\mathbf{g}_1 & \cdots & \mathbf{g}_m & [\mathbf{f},\mathbf{g}_1] & \cdots & [\mathbf{f},\mathbf{g}_m] & \cdots & \left(ad_{\mathbf{f}}^k,\mathbf{g}_1\right) & \cdots & \left(ad_{\mathbf{f}}^k,\mathbf{g}_m\right)\end{bmatrix} \quad \text{(Eq. 69)}$$

is n. For the current system sub-matrix of Eq. 69 $[\mathbf{g}_1 \quad \mathbf{g}_2 \quad \mathbf{g}_3]$ already have rank 3. In order to have full rank, it is necessary to find a linearly independent column in the rest of the columns. It is first proved that all the first order Lie bracket columns are linear dependent on the basic columns $[\mathbf{g}_1 \quad \mathbf{g}_2 \quad \mathbf{g}_3]$. In order for the column to be

$$\begin{aligned}
[\mathbf{f},\mathbf{g}_1] &= \nabla\mathbf{g}_1\times\mathbf{f}-\nabla\mathbf{f}\times\mathbf{g}_1=-\nabla\mathbf{f}\times\mathbf{g}_1=-\begin{bmatrix}0 & \dfrac{x_3 i_2\eta}{R\left(\dfrac{\left(J_1x_3^2+J_2\right)i_2^2+J_3}{R^2}+m\right)} & 0 & 0\end{bmatrix}^T \\
[\mathbf{f},\mathbf{g}_2] &= \nabla\mathbf{g}_2\times\mathbf{f}-\nabla\mathbf{f}\times\mathbf{g}_2=-\nabla\mathbf{f}\times\mathbf{g}_2=-\begin{bmatrix}0 & 0 & L_{\mathbf{g}_2}\left(L_{\mathbf{f}}^1h_1\right) & 0\end{bmatrix}^T \\
[\mathbf{f},\mathbf{g}_3] &= \nabla\mathbf{g}_3\times\mathbf{f}-\nabla\mathbf{f}\times\mathbf{g}_3=-\nabla\mathbf{f}\times\mathbf{g}_3=-\begin{bmatrix}0 & 0 & 0 & \dfrac{-1}{R\left(\dfrac{\left(J_1x_3^2+J_2\right)i_2^2+J_3}{R^2}+m\right)}\end{bmatrix}^T
\end{aligned} \quad \text{(Eq. 70)}$$

[00149] The second order Lie bracket can be represented as

$$\begin{aligned}
\left[\mathbf{f},[\mathbf{f},\mathbf{g}_1]\right] &= \nabla[\mathbf{f},\mathbf{g}_1]\times\mathbf{f}-\nabla\mathbf{f}\times[\mathbf{f},\mathbf{g}_1]=-\nabla\mathbf{f}\times[\mathbf{f},\mathbf{g}_1] \\
\left[\mathbf{f},[\mathbf{f},\mathbf{g}_2]\right] &= \nabla[\mathbf{f},\mathbf{g}_2]\times\mathbf{f}-\nabla\mathbf{f}\times[\mathbf{f},\mathbf{g}_2] \\
\left[\mathbf{f},[\mathbf{f},\mathbf{g}_3]\right] &= \nabla[\mathbf{f},\mathbf{g}_3]\times\mathbf{f}-\nabla\mathbf{f}\times[\mathbf{f},\mathbf{g}_3]=-\nabla\mathbf{f}\times[\mathbf{f},\mathbf{g}_3]
\end{aligned} \quad \text{(Eq. 71)}$$

[00150] Among all the second order Lie bracket, column $\left[\mathbf{f},[\mathbf{f},\mathbf{g}_2]\right]$ is linearly independent with respect to basic columns. As a result the controllability of the nonlinear system in Eq. 61 is strictly proved.

[00151] **D. Nonlinear Coordinate Transformation**

[00152] Assuming the following nonlinear coordinate transformation

$$\boldsymbol{\xi}=\begin{bmatrix}\xi_1\\ \xi_2\\ \xi_3\\ \xi_4\end{bmatrix}=\boldsymbol{\Phi}(\mathbf{x})=\begin{bmatrix}h_1\\ L_{\mathbf{f}}^1 h_1\\ h_2\\ h_3\end{bmatrix}=\begin{bmatrix} x_1 \\ \dfrac{x_2 x_3 i_2 \eta - x_4}{R} - mg\sin(d) - \dfrac{1}{2}\rho C_d A x_1^2 \\ \dfrac{-m\cos(d)\,g\left(R_{c0}+R_{c1}x_1\right)\left(\dfrac{2}{1+\exp(-40x_1)}-1\right)}{\dfrac{\left(J_1 x_3^2+J_2\right)i_2^2+J_3}{R^2}+m} \\ x_2 \\ x_3 \end{bmatrix} \quad \text{(Eq. 72)}$$

its derivative can be obtained as follows

$$\begin{aligned}\dot{\xi}_1 &= \frac{\dfrac{x_2 x_3 i_2 \eta - x_4}{R} - mg\sin(d) - \dfrac{1}{2}\rho C_d A x_1^2}{\dfrac{-m\cos(d)\,g\left(R_{c0}+R_{c1}x_1\right)\left(\dfrac{2}{1+\exp(-40x_1)}-1\right)}{\dfrac{\left(J_1 x_3^2+J_2\right)i_2^2+J_3}{R^2}+m}} = L_{\mathbf{f}}^1 h_1 \\ \dot{\xi}_2 &= L_{\mathbf{f}}^2 h_1 + L_{\mathbf{g}_1}\left(L_{\mathbf{f}}^1 h_1\right)u_1 + L_{\mathbf{g}_2}\left(L_{\mathbf{f}}^1 h_1\right)u_2 + L_{\mathbf{g}_3}\left(L_{\mathbf{f}}^1 h_1\right)u_3 \\ \dot{\xi}_3 &= L_{\mathbf{f}}^2 h_2 + u_1 \\ \dot{\xi}_4 &= L_{\mathbf{f}}^2 h_3 + u_2\end{aligned} \quad \text{(Eq. 73)}$$

[00153] Using the nonlinear coordinate transformation in Eq. 72, Eq. 73 can be rewritten in its Byrnes-Isidori normal form

$$\begin{aligned}\dot{\xi}_1 &= \xi_2 \\ \begin{bmatrix}\dot{\xi}_2\\ \dot{\xi}_3\\ \dot{\xi}_4\end{bmatrix} &= \boldsymbol{\alpha}(\boldsymbol{\xi})+\boldsymbol{\beta}(\boldsymbol{\xi})\begin{bmatrix}u_1\\ u_2\\ u_3\end{bmatrix}\end{aligned} \quad \text{(Eq. 74)}$$

$$\boldsymbol{\alpha}(\boldsymbol{\xi})=\begin{bmatrix}L_{\mathbf{f}}^2 h_1\\ 0\\ 0\end{bmatrix},\ \boldsymbol{\beta}(\boldsymbol{\xi})=\begin{bmatrix}L_{\mathbf{g}_1}\left(L_{\mathbf{f}}^1 h_1\right) & L_{\mathbf{g}_2}\left(L_{\mathbf{f}}^1 h_1\right) & L_{\mathbf{g}_3}\left(L_{\mathbf{f}}^1 h_1\right)\\ 1 & 0 & 0\\ 0 & 1 & 0\end{bmatrix}$$

[00154] Using the static feedback control law

$$\mathbf{u} = \boldsymbol{\beta}(\boldsymbol{\xi})^{-1}\left(\mathbf{v} - \boldsymbol{\alpha}(\boldsymbol{\xi})\right), \qquad \boldsymbol{\alpha}(\boldsymbol{\xi}) + \boldsymbol{\beta}(\boldsymbol{\xi})\mathbf{u} = \mathbf{v} \tag{Eq. 75}$$

system in equation Eq. 73 can be rewritten in its linearized canonical form

$$\begin{bmatrix} \dot{\xi}_1 \\ \dot{\xi}_2 \\ \dot{\xi}_3 \\ \dot{\xi}_4 \end{bmatrix} = \mathbf{A}\begin{bmatrix} \xi_1 \\ \xi_2 \\ \xi_3 \\ \xi_4 \end{bmatrix} + \mathbf{B}\begin{bmatrix} v_1 \\ v_2 \\ v_3 \end{bmatrix}$$
$$\mathbf{A} = \begin{bmatrix} 0 & 1 & 0 & 0 \\ 0 & 0 & 0 & 0 \\ 0 & 0 & 0 & 0 \\ 0 & 0 & 0 & 0 \end{bmatrix}, \quad \mathbf{B} = \begin{bmatrix} 0 & 0 & 0 \\ 1 & 0 & 0 \\ 0 & 1 & 0 \\ 0 & 0 & 1 \end{bmatrix} \tag{Eq. 76}$$

[00155] **E. Feedback Controller Architecture and Controller Design**

[00156] It is noticed that the linearized system in Eq. 76 is open loop unstable because the eigenvalue of the open loop system is on the imaginary axis. Therefore, it may be necessary to design a feedback controller to stabilize the system and enable the tracking of a desired trajectory of states of the system. Figure 11 illustrates the architecture of the nonlinear adaptive cruise controller 232 according to certain embodiments of the present technology, while Figure 12 provides the mathematical embodiment. In Figure 11, two nonlinear coordinate transformations are applied to convert the real physical world state vector into a linearized state vector. Further, a decoupling controller is used to convert the linearized-decoupled control input into the real physical world control input. In this way, the sequential connection of decoupling controller, nonlinear plant model and nonlinear coordinate transformation becomes the essentially linear system in Eq. 76. According to such embodiments, the controller shown by the controller block in Figure 12 may be configured to stabilize and enable for tracking of the desired trajectory.

[00157] The nonlinear adaptive cruise controller 232 also includes a linear-quadratic-Gaussian (LQG) controller 240. After the converting of the global linearized system is achieved, the LQG controller 240 may be configured to achieve optimal trajectory tracking of all observable and controllable states, such as, for example, vehicle

speed, vehicle distance, and engine torque. Thus, instead of calculating linear controller gain or leaving the controller gain to an engine controller, the smart cruise control system 210 uses the combination of nonlinear transformations and Linear Quadratic Gaussian (LQG) to achieve true optimal feedback control.

[00158] The trajectory tracking information from the LQG controller 240 may then be provided to the nonlinear inputs transformation block 238, which converts transformed states into inputs, before information regarding the control inputs, such as the control inputs changing rates (u_1, u_2, u_3) and they are the extended inputs of Eq. 61, are provided to an integrator block 242. The integrator block 242 enables the design of global linearization of non-affine-nonlinear system by converting the general nonlinear system into its affine nonlinear form. The integrator block 242 integrates the control inputs changing rates and then provides the control inputs to the non-linear vehicle plant 245, such as, for example, an electronic control unit for the engine and/or an electronic control unit for the transmission of the vehicle 200.

[00159] Designing the controller in Figure 12 may be the same as designing an optimal controller for a pure linear system. The Linear Quadratic Gaussian (LQG) set point may be selected as the design methodology. In this configuration, the state-space model of the process may have the form

$$\dot{\boldsymbol{\xi}} = \mathbf{A}\boldsymbol{\xi} + \mathbf{B}\mathbf{v}, \qquad \boldsymbol{\gamma} = \mathbf{C}\boldsymbol{\xi}, \qquad \mathbf{z} = \mathbf{G}\boldsymbol{\xi} + \mathbf{H}\mathbf{v}. \qquad \text{(Eq. 77)}$$

where $\boldsymbol{\gamma}$ is the measured output in the linearized state space and $\mathbf{z}$ will be the output that will be controlled. While matrix $\mathbf{A}$ and $\mathbf{B}$ are already defined in Eq. 76, the rest of the matrices are defined as

$$\mathbf{C} = \mathbf{I}_{4\times 4}, \quad \mathbf{G} = \begin{bmatrix} 1 & 0 & 0 & 0 \\ 0 & 0 & 1 & 0 \\ 0 & 0 & 0 & 1 \end{bmatrix}, \quad \mathbf{H} = \begin{bmatrix} 0 & 0 & 0 \\ 0 & 0 & 0 \\ 0 & 0 & 0 \end{bmatrix}. \qquad \text{(Eq. 78)}$$

[00160] The value of matrix $\mathbf{G}$ means that the controlled output is vehicle speed, engine torque, and gear ratio. Since it is noticed that $\mathbf{H}^T\mathbf{G} = 0$, Kalman's inequity may mean that the LQG controller 240 will be sufficiently robust for a certain amount of multiplicative uncertainty. According to certain embodiments, the LQG controller 240

may consist of the one Linear Quadratic Regulator (LQR), one LQG estimator and the definition of set point, as shown in Figure 13.

[00161] Optimal LQR

[00162] The optimal LQR problem is defined generally and consists of finding the matrix gain $\mathbf{K}$ controller that minimizes

$$\begin{aligned} J_{LQR} &= \int_0^\infty \left(\mathbf{z}'\mathbf{Q}\mathbf{z} + \mathbf{v}'\mathbf{R}\mathbf{v}\right) dt \\ &= \int_0^\infty \left(\mathbf{x}\mathbf{G}'\mathbf{Q}\mathbf{G}\mathbf{x}' + \mathbf{v}'\left(\mathbf{H}'\mathbf{Q}\mathbf{H} + \mathbf{R}\right)\mathbf{v}\right) dt \\ &= \int_0^\infty \left(\mathbf{x}\mathbf{G}'\mathbf{Q}\mathbf{G}\mathbf{x}' + \mathbf{v}'\mathbf{R}\mathbf{v}\right) dt \end{aligned} \qquad \text{(Eq. 79)}$$

where $\mathbf{Q}$ is a 3×3 symmetric positive-definite matrix, and $\mathbf{R}$ is a 3×3 symmetric positive definite matrix. The optimal LQR gain matrix is

$$\mathbf{K} = \mathbf{R}^{-1}\mathbf{B}^T\mathbf{P} \qquad \text{(Eq. 80)}$$

where $\mathbf{P}$ is the solution of the Algebraic Riccati Equation (ARE)

$$\mathbf{A}^T\mathbf{P} + \mathbf{P}\mathbf{A} - \mathbf{P}\mathbf{B}\mathbf{R}^{-1}\mathbf{B}^T\mathbf{P} + \mathbf{G}'\mathbf{Q}\mathbf{G} = \mathbf{0}. \qquad \text{(Eq. 81)}$$

[00163] Optimal LQG

[00164] The optimal LQG estimator is defined as finding the matrix gain $\mathbf{L}$ that minimizes the asymptotic expected value of the estimator error

$$J_{LQG} = \lim_{t\to\infty} \mathbf{E}\left(\left\|\xi - \hat{\xi}\right\|^2\right) \qquad \text{(Eq. 82)}$$

with zero-mean Gaussian noise process $\mathbf{Q}_N$ and $\mathbf{R}_N$. The optimal LQG estimator gain $\mathbf{L}$ is the matrix given by

$$\mathbf{L} = \mathbf{S}\mathbf{C}\mathbf{R}_N^{-1} \qquad \text{(Eq. 83)}$$

and $\mathbf{S}$ is the unique positive definite solution to the following

$$\mathbf{A}\mathbf{S} + \mathbf{S}\mathbf{A}' + \mathbf{B}\mathbf{Q}_N\mathbf{B}' - \mathbf{S}\mathbf{C}'\mathbf{R}_N^{-1}\mathbf{C}\mathbf{S} = \mathbf{0} \qquad \text{(Eq. 84)}$$

[00165] Set Point Definition

[00166] When one does not want $\mathbf{z}$ as small as possible, but instead make it converge as fast as possible to a given constant set-point value $\mathbf{r}$, the state ξ and input $\mathbf{v}$ of process Eq. 77 may be made to converge to value ξ^* and $\mathbf{v}^*$ for which

$$0 = \mathbf{A}\xi^* + \mathbf{B}\mathbf{v}^*, \qquad 0 = \mathbf{G}\xi^* + \mathbf{H}\mathbf{v}^*. \qquad \text{(Eq. 85)}$$

The solution to this equation is

$$\begin{bmatrix} \xi^* \\ \mathbf{v}^* \end{bmatrix} = \begin{bmatrix} \mathbf{A} & \mathbf{B} \\ \mathbf{G} & \mathbf{H} \end{bmatrix}^{-1} \begin{bmatrix} \mathbf{0} \\ \mathbf{r} \end{bmatrix} = \begin{bmatrix} \mathbf{F} \\ \mathbf{N} \end{bmatrix} \mathbf{r} \qquad \text{(Eq. 86)}$$

[00167] As shown in Figure 3, the smart cruise control system 210 also includes a vehicle parameter estimator block 244 that provides estimations of vehicle parameters for use by a variety of components of the smart cruise control system 210, including, for example, the adaptive optimal control system 216 and the nonlinear adaptive cruise controller 232. According to certain embodiments, as illustrated in Figure 14, the vehicle parameter estimator block 244 includes normal mode and degenerated mode joint unscented or extended Kalman filters 246a, 246b based algorithm that estimates vehicle mass, aerodynamic drag, and rolling coefficient based on the input-output relationship of the vehicle dynamics when the vehicle positioning and horizon generation system 214 is functional in normal mode, *e.g.,* when the map data is available. According to certain embodiments, such estimates may be based on information from sensor inputs.

[00168] While Figure 14 refers to joint unscented Kalman filters 246a, 246b, according to other embodiments, the filters 246a, 246b may be dual or joint extended Kalman filters, or a dual unscented Kalman filter, among others. However, unlike an extended Kalman filter, an unscented Kalman filter may be used to achieve a second order approximation. Additionally, unlike an extended Kalman filter, an unscented Kalman filter does not require the explicitly calculation of Jacobian matrix.

[00169] Figure 21 illustrates an embodiment of a smart cruise control platform 250 at the concept evaluation stage that uses on-vehicle navigation sensors 212 such as GPS and IMU that are configured to receive signals relating to the position or location of the vehicle 200. The smart cruise control platform 250 includes a prototyping laptop 251 that

includes a smart cruise control system 253. Although Figure 21 illustrates a vehicle parameter estimator 256 separate from the smart cruise control system 253, similar to the smart cruise control system 210 shown in Figure 3, the vehicle parameter estimator 256 may also be part of the smart cruise control system 253 shown in Figure 21. Additionally, according to certain embodiments, the smart cruise control platform 250 may use an Advanced Driver Assistance Systems Research Platform (ADAS RP) 254, such as, for example, commercially available ADAS RP software from Nokia, to provide a three-dimensional map data, and to conduct the sensor data fusion, map matching, and electronic road horizon generation.

[00170] Figure 22 illustrates an embodiment of a smart cruise control platform 252 at the production stage that includes on-vehicle navigation sensors 212 such as, for example, GPS and IMU. The smart cruise control platform 252 also includes an electronic control module (ECM) 255 that includes a smart cruise control system 253, a vehicle positioning and horizon generation system 214, and a vehicle parameter estimator 256. The vehicle positioning and horizon generation system 214 has access to a three-dimensional map or terrain database 211 of terrain and/or road information. The vehicle positioning and horizon generation system 214 uses the terrain information as well as positional information received by the on-vehicle navigation sensors 212 to provide an estimated road horizon. The estimated road horizon may provide a variety of information, such as, for example, current and/or upcoming road grades and curvatures and the lengths of such road characteristics, as well as the distance before the vehicle 200 reaches changes in road grade and curvature. The estimated road horizon may be provided to a vehicle parameter estimator block 256, which may estimate vehicle mass, aero dynamic drag, and rolling resistance based on input from one or more vehicle state sensors 258.

[00171] As shown in Figures 21 and 22, a vehicle CAN bus 260, or vector CAN hardware, may be used for communicating information from vehicle state the sensors 258 to the smart cruise control system 253, such as, for example, sensed information pertaining to a wheel speed, engine speed, engine torque, and current gear, among other information. Additionally, the vehicle CAN bus 260, or vector CAN hardware, may be used for communicating information from the smart cruise control system 253 to the vehicle CAN bus 260, such as to the ECU of the vehicle 200, including, for example, the

engine ECU 260a and/or the transmission ECU 260b. The ECU(s) 260a, 260b may then send information to the engine 266 or transmission 264 associated with that particular ECU 260a, 260b, such as commands pertaining to set speed, gear shifting, engine torque, and engine brake commands. These commands may adjust the engine torque and engine brake torque in the vehicle engine, and control the gear shifting in the vehicle transmission based on the predicted road information to follow the optimal vehicle speed calculated from the nonlinear optimization block 218 to minimize the defined cost function in Eq. 8. Additionally, the smart cruise control system 210 and/or smart cruise control platform 250, 252 of a vehicle 200 may be configured to receive information from the smart cruise control system 210 of another vehicle 200. For example, referencing Figure 23, a first vehicle 200a is in the horizon of a second vehicle 200b. According to such an embodiment, the smart cruise control systems 210 of the first and second vehicles 200a, 200b may each be operably connected to a transceiver 268 that allow for the smart cruise control systems 210 on the first and second vehicles 200a, 200b to communicate. Therefore, the smart cruise control system 210 on the first vehicle 200a may be able to provide information, such as traffic condition, to the second vehicle 200b. In such circumstances, information pertaining to the road profile being traveled on by the first vehicle 200a may be transmitted through the transceiver 268 to the second vehicle 200b and used by the smart cruise control system 210 of the second vehicle 200b to control the operation of the transmission 264 or engine 266.

[00172] Figures 24 and 25 illustrate radar enabled smart cruise control systems 270a, 270b. As shown, the radar enabled smart cruise control system 270a in Figure 24 is similar to the smart cruise control system 210 shown in Figure 3 with the exception of the addition of a radar system 272. The radar system 272, which includes one or more radars, provides information that allows for onboard radar measurements by the radar system 272, such as radar range and rate range measurements (relative distance and speed) between the vehicle 200 having the radar enabled smart cruise control system 270a, 270b and leading and/or following vehicles. The information from radar system 272 may be sent to the adaptive optimal control system 216 to be used as an extra constraint in the nonlinear optimization block 218 to calculate fuel optimal control inputs. Moreover, information from the radar system 272 may be used to generate an adaptive speed trace

based on both road grade and traffic to reduce fuel consumption. To achieve this goal, the smart cruise control algorithm of the nonlinear optimization block 218 may be modified to use the existing Adaptive Cruise Control (ACC) forward-looking radar and an additional low-cost backward-looking radar or camera to measure the range and range-rate (relative distance and speed) between the vehicle 200 and leading and following vehicles. The control objectives may include calculating the optimal set speed and gear shifting, and using the surrounding traffic interaction as constraints such as driver rider comfort which evaluates the comfort of the driver of the vehicle 200, driver safe tracking range which is the safe relative distance for the following vehicle, and front/rear-end safety (also referred to the safe distance between vehicles). Such control objectives may allow for the vehicle 200 to be maintained at a safe distance between following and/or leading vehicles while the vehicle 200 is cruising at or near the smart cruise control system set speed as much as possible to maximize the gain of fuel economy.

CLAIMS

1. A method for controlling the operation of a vehicle that has a transmission and an engine using a predictive control system, the method comprising:

predicting a characteristic of a portion of a road;

defining a cost function based on a plurality of vehicle parameters and the predicted road characteristic;

calculating, based at least in part on the predicted road characteristic and on minimizing the defined cost function, an engine torque command for the operation of the engine;

calculating, based at least in part on the predicted road characteristic and on minimizing the defined cost function, an engine brake torque command for operation of the engine;

calculating, based at least in part on the predicted road characteristic and on minimizing the defined cost function, a vehicle set speed;

determining, based at least in part on the predicted road characteristic and on minimizing the defined cost function, a gear shifting command for operation of the transmission;

transmitting a signal representative of the gear shifting command to an electronic control unit associated with the transmission; and

adjusting the engine torque command, the engine brake torque command, and the gear shifting command based on the predicted road characteristic to follow the calculated vehicle set speed to minimize the defined cost function.

2. The method of claim 1, further including the step of adjusting the engine torque and the vehicle set speed based on differences between the road characteristic of a first portion of the road on which the vehicle is positioned and the road characteristic of a second portion of the road that the vehicle is approaching.

3. The method of claim 2, wherein the adjustment of the engine torque and the vehicle set speed occurs before the vehicle reaches the second portion of the road.

4. The method of claim 3, wherein the predicted road characteristic includes predicting a slope and a curvature of the road.

5. The method of claim 1, further including the steps of estimating a value for the plurality of vehicle parameters as the vehicle travels along the road, and adjusting the value as the value changes during operation of the vehicle, the plurality of vehicle parameters including at least one of the following: vehicle mass, aerodynamic drag, or rolling resistance.

6. The method of claim 5, wherein the steps of calculating the engine torque command and the vehicle set speed and determining the gear shifting command are at least in part also based on the value of the plurality of vehicle parameters.

7. The method of claim 6, further including the step of calculating, based at least in part on the estimated value of the vehicle parameters, an engine torque command, and adjusting the speed of the vehicle based at least in part on the calculated engine torque command.

8. The method of claim 1, wherein the steps of calculating the engine torque command and the vehicle set speed and determining gear shifting command are at least in part also based on a speed of the wind that is approximately along or against a vehicle heading angle.

9. The method of claim 1, wherein the steps of calculating the engine torque command and the vehicle set speed and determining gear shifting command are at least in part also based on a legal speed limit of a portion of the road, and wherein the calculated engine torque command and the vehicle set speed and determining gear shifting command are adjusted based on a change in the legal speed limit for the portion of the road the vehicle is approaching.

10. The method of claim 1, wherein the steps of calculating the engine torque command and the vehicle set speed and determining gear shifting command are at least in part also based on either or both a real time traffic condition and a historical traffic condition.

11. The method of claim 10, wherein the step of calculating the engine brake torque command is also based on either or both the real time traffic condition and the historical traffic condition.

12. The method of claim 1, wherein the step of predicting the road characteristic includes determining the location of the vehicle, the determination of the location of the vehicle being based at least in part on data from a Global Positioning System, an odometer, and an inertial measurement unit, the inertial measurement unit including a gyroscope and an accelerometer.

13. The method of claim 12, wherein the step of predicting the road characteristic further includes enabling dead reckoning navigation when data from the Global Positioning System is unavailable to determine the location of the vehicle, the dead reckoning navigation being based at least in part on information provided by the odometer and the inertial measurement unit.

14. The method of claim 12, wherein the step of determining the location of the vehicle further includes:

combining the data from the Global Positioning System, the odometer, and the inertial measurement unit in a sensor fusion system;

estimating a Global Positioning System sensor error parameter;

estimating an inertial measurement unit sensor error parameter; and

feeding the estimated Global Positioning System sensor error parameter and the estimated inertial measurement unit sensor error parameter to the sensor fusion system to improve the accuracy of the determination of the location of the vehicle.

15. The method of claim 1, further including the step of transmitting data regarding a portion of the road travelled on by the vehicle to another vehicle that is approaching that same portion of road, the transmitted data at least assisting in controlling the operation of the other vehicle when the vehicle travels along that same portion of road.

AMENDED CLAIMS
received by the International Bureau on 01 July 2013 (01.07.2013)

1. A method for controlling the operation of a vehicle that has a transmission and an engine using a predictive control system, the method comprising:

predicting a characteristic of a portion of a road;

defining a cost function based on a plurality of vehicle parameters and the predicted road characteristic;

calculating, based at least in part on the predicted road characteristic and on minimizing the defined cost function, an engine torque command for the operation of the engine;

calculating, based at least in part on the predicted road characteristic and on minimizing the defined cost function, an engine brake torque command for operation of the engine;

calculating, based at least in part on the predicted road characteristic and on minimizing the defined cost function, a vehicle set speed;

determining, based at least in part on the predicted road characteristic and on minimizing the defined cost function, a gear shifting command for operation of the transmission;

transmitting a signal representative of the gear shifting command to an electronic control unit associated with the transmission; and

adjusting the engine torque command, the engine brake torque command, and the gear shifting command based on the predicted road characteristic to follow the calculated vehicle set speed to minimize the defined cost function, wherein the step of predicting the road characteristic includes determining the location of the vehicle, the determination of the location of the vehicle being based at least in part on data from a Global Positioning System, an odometer, and an inertial measurement unit, the inertial measurement unit including a gyroscope and an accelerometer.

2. The method of claim 1, further including the step of adjusting the engine torque and the vehicle set speed based on differences between the road characteristic of a first portion of the

road on which the vehicle is positioned and the road characteristic of a second portion of the road that the vehicle is approaching.

3. The method of claim 2, wherein the adjustment of the engine torque and the vehicle set speed occurs before the vehicle reaches the second portion of the road.

4. The method of claim 3, wherein the predicted road characteristic includes predicting a slope and a curvature of the road.

5. The method of claim 1, further including the steps of estimating a value for the plurality of vehicle parameters as the vehicle travels along the road, and adjusting the value as the value changes during operation of the vehicle, the plurality of vehicle parameters including at least one of the following: vehicle mass, aerodynamic drag, or rolling resistance.

6. The method of claim 5, wherein the steps of calculating the engine torque command and the vehicle set speed and determining the gear shifting command are at least in part also based on the value of the plurality of vehicle parameters.

7. The method of claim 6, further including the step of calculating, based at least in part on the estimated value of the vehicle parameters, an engine torque command, and adjusting the speed of the vehicle based at least in part on the calculated engine torque command.

8. The method of claim 1, wherein the steps of calculating the engine torque command and the vehicle set speed and determining gear shifting command are at least in part also based on a speed of the wind that is approximately along or against a vehicle heading angle.

9. The method of claim 1, wherein the steps of calculating the engine torque command and the vehicle set speed and determining gear shifting command are at least in part also based on a legal speed limit of a portion of the road, and wherein the calculated engine torque command and the vehicle set speed and determining gear shifting command are adjusted based on a change in the legal speed limit for the portion of the road the vehicle is approaching.

10. The method of claim 1, wherein the steps of calculating the engine torque command and the vehicle set speed and determining gear shifting command are at least in part also based on either or both a real time traffic condition and a historical traffic condition.

11. The method of claim 10, wherein the step of calculating the engine brake torque command is also based on either or both the real time traffic condition and the historical traffic condition.

12. The method of claim 1, wherein the step of predicting the road characteristic further includes enabling dead reckoning navigation when data from the Global Positioning System is unavailable to determine the location of the vehicle, the dead reckoning navigation being based at least in part on information provided by the odometer and the inertial measurement unit.

13. The method of claim 1, wherein the step of determining the location of the vehicle further includes:

combining the data from the Global Positioning System, the odometer, and the inertial measurement unit in a sensor fusion system;

estimating a Global Positioning System sensor error parameter;

estimating an inertial measurement unit sensor error parameter; and

feeding the estimated Global Positioning System sensor error parameter and the estimated inertial measurement unit sensor error parameter to the sensor fusion system to improve the accuracy of the determination of the location of the vehicle.

14. The method of claim 1, further including the step of transmitting data regarding a portion of the road travelled on by the vehicle to another vehicle that is approaching that same portion of road, the transmitted data at least assisting in controlling the operation of the other vehicle when the vehicle travels along that same portion of road.

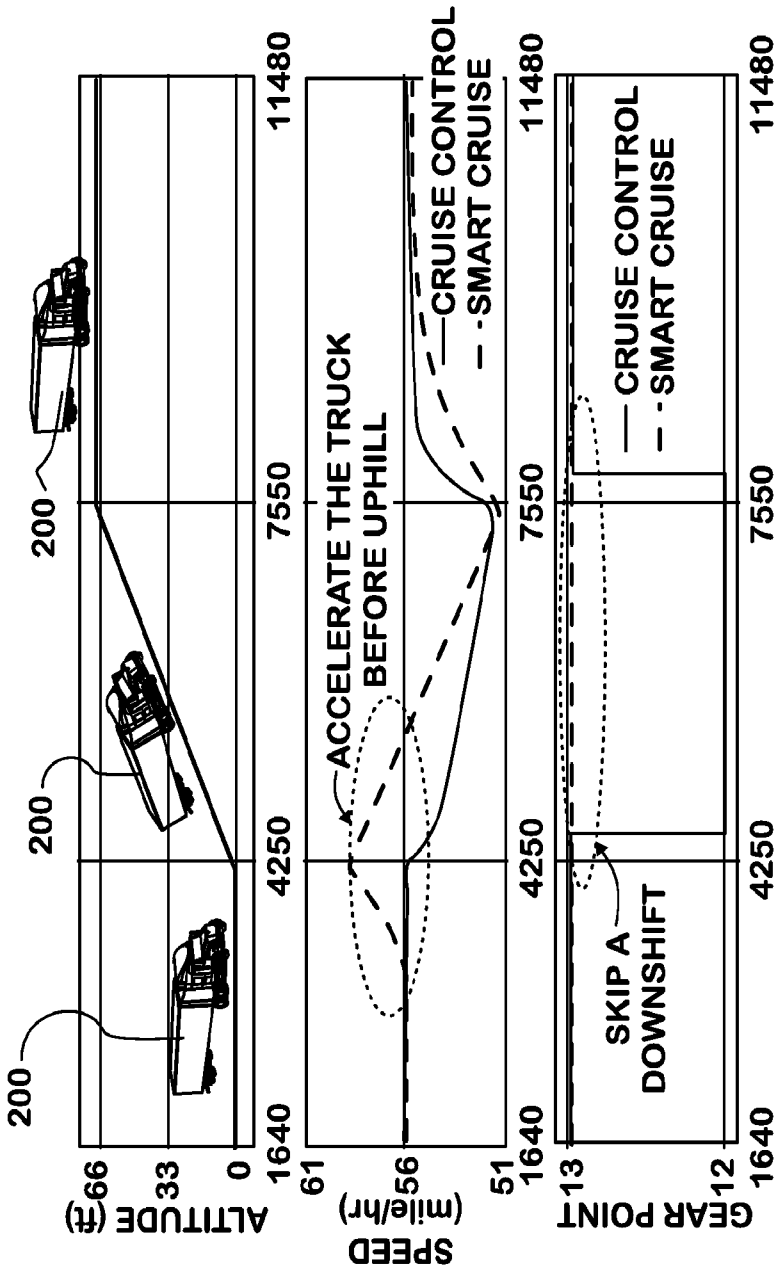
ALTITUDE (ft)
99
66
33
0
SPEED (mile/hr)
61
56
51
GEAR POINT
13
12
1640
4250
7550
11480
DISTANCE (ft)
200
200
200
ACCELERATE THE TRUCK BEFORE UPHILL
CRUISE CONTROL
SMART CRUISE
SKIP A DOWNSHIFT

FIG. 1

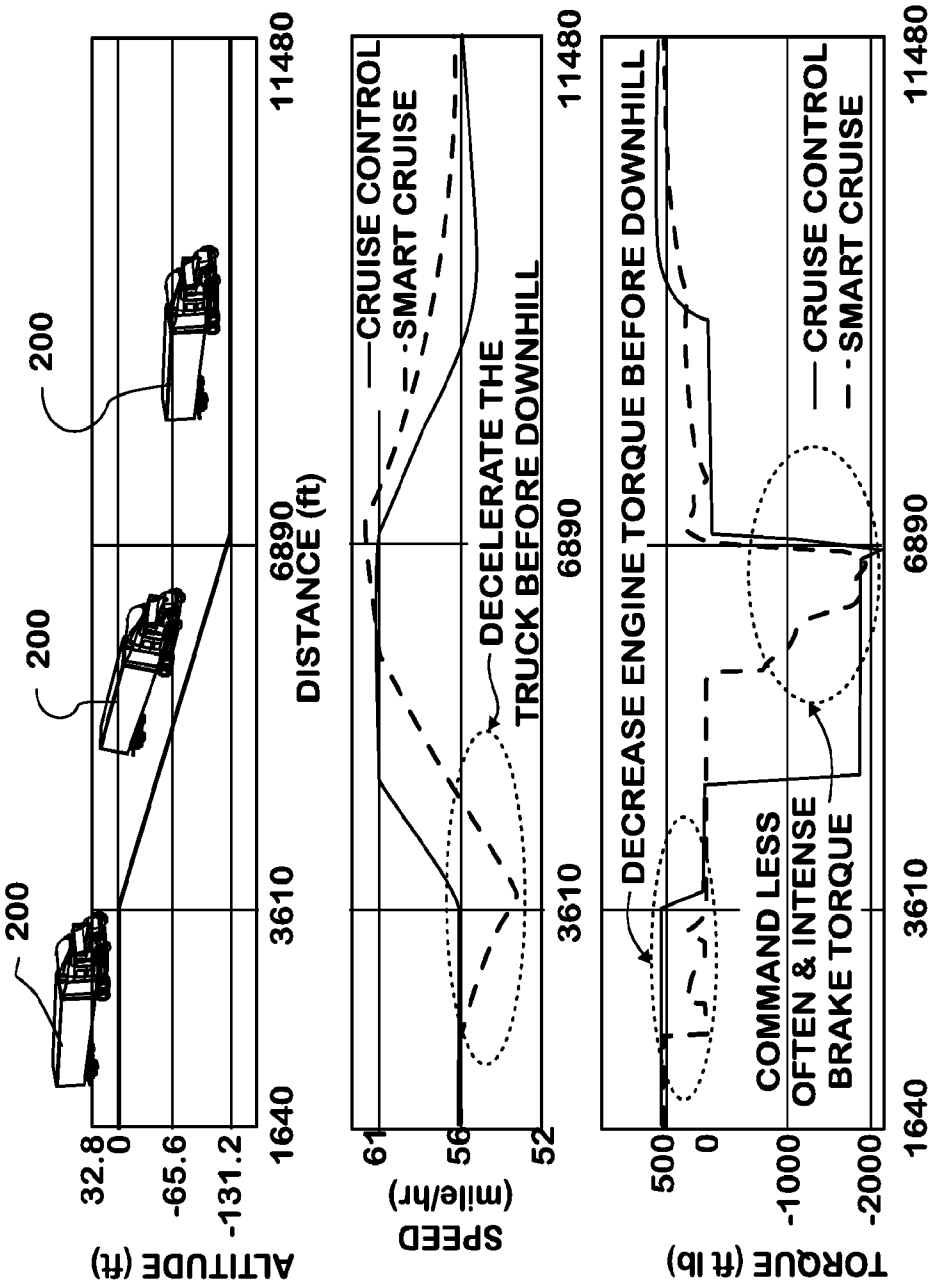
200
200
200
ALTITUDE (ft)
32.8
0
-65.6
-131.2
1640
3610
6890
11480
DISTANCE (ft)
SPEED (mile/hr)
61
56
52
CRUISE CONTROL
SMART CRUISE
DECELERATE THE TRUCK BEFORE DOWNHILL
TORQUE (ft lb)
500
0
-1000
-2000
DECREASE ENGINE TORQUE BEFORE DOWNHILL
COMMAND LESS OFTEN & INTENSE BRAKE TORQUE

FIG. 2

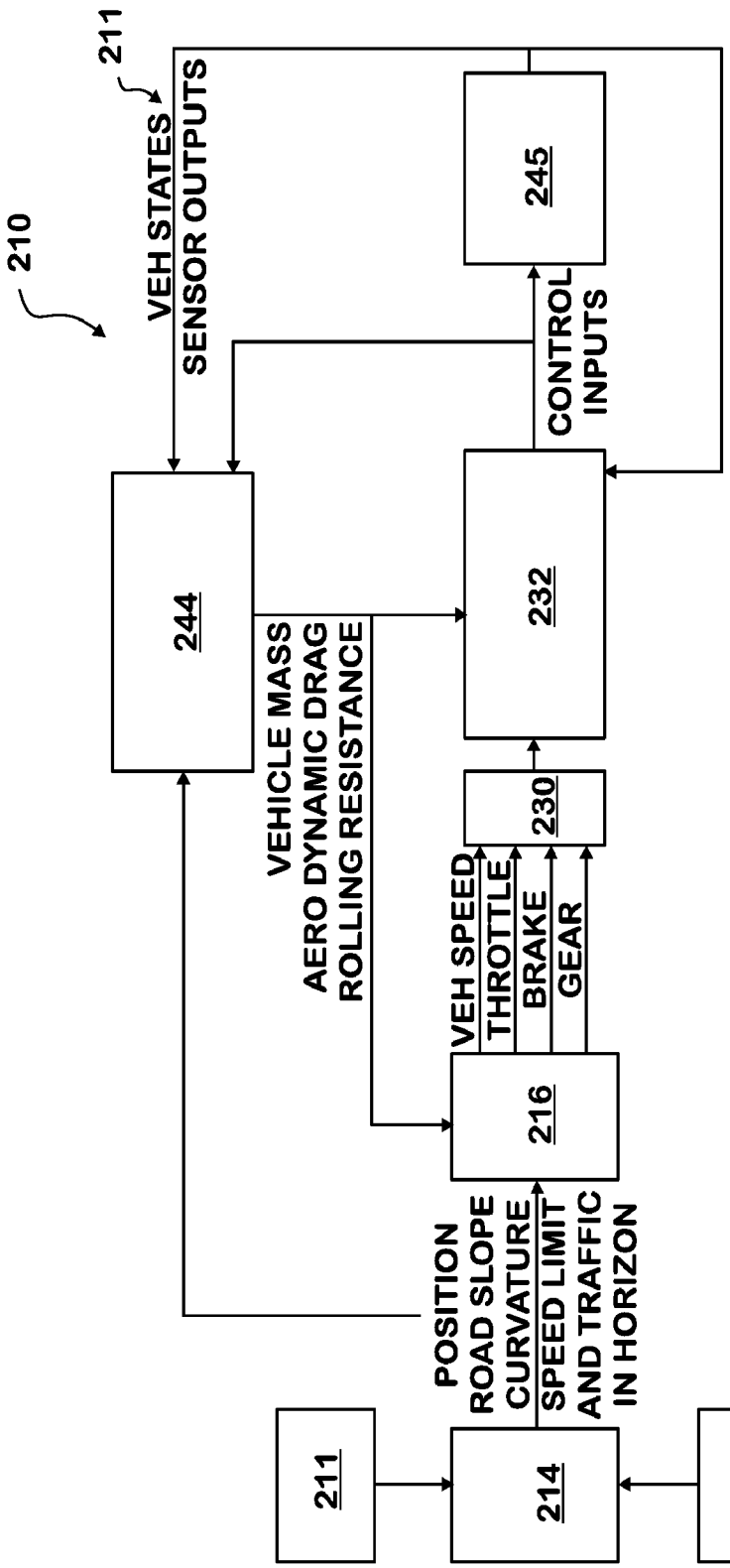
210
211
VEH STATES
SENSOR OUTPUTS
245
CONTROL INPUTS
244
232
VEHICLE MASS
AERO DYNAMIC DRAG
ROLLING RESISTANCE
230
VEH SPEED
THROTTLE
BRAKE
GEAR
216
POSITION
ROAD SLOPE
CURVATURE
SPEED LIMIT
AND TRAFFIC
IN HORIZON
211
214
212

FIG. 3

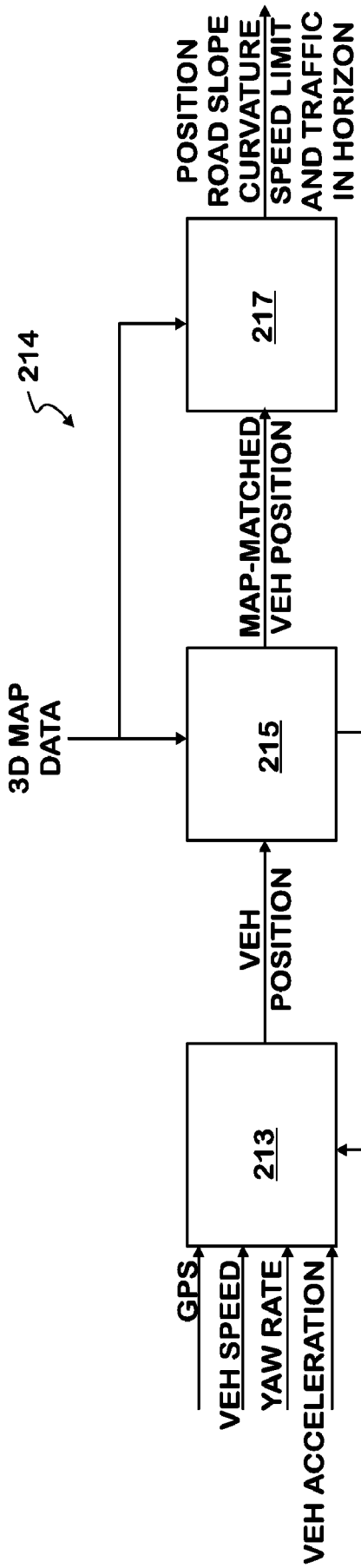
GPS
VEH SPEED
YAW RATE
VEH ACCELERATION
213
VEH POSITION
ESTIMATED GPS & IMU ERROR PARAMETERS
3D MAP DATA
215
MAP-MATCHED VEH POSITION
214
217
POSITION ROAD SLOPE CURVATURE SPEED LIMIT AND TRAFFIC IN HORIZON

FIG. 4

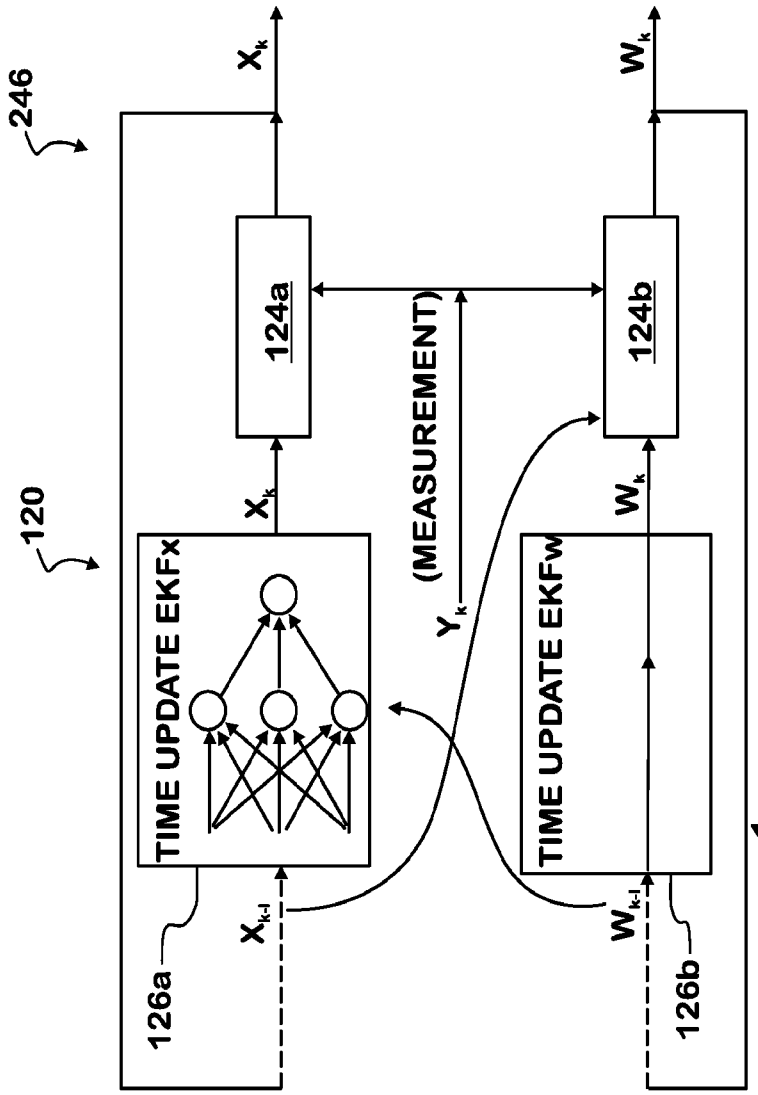
246
120
X_k
W_k
124a
124b
(MEASUREMENT)
Y_k
TIME UPDATE EKFx
TIME UPDATE EKFw
X_{k-1}
W_{k-1}
126a
126b
122

FIG. 5

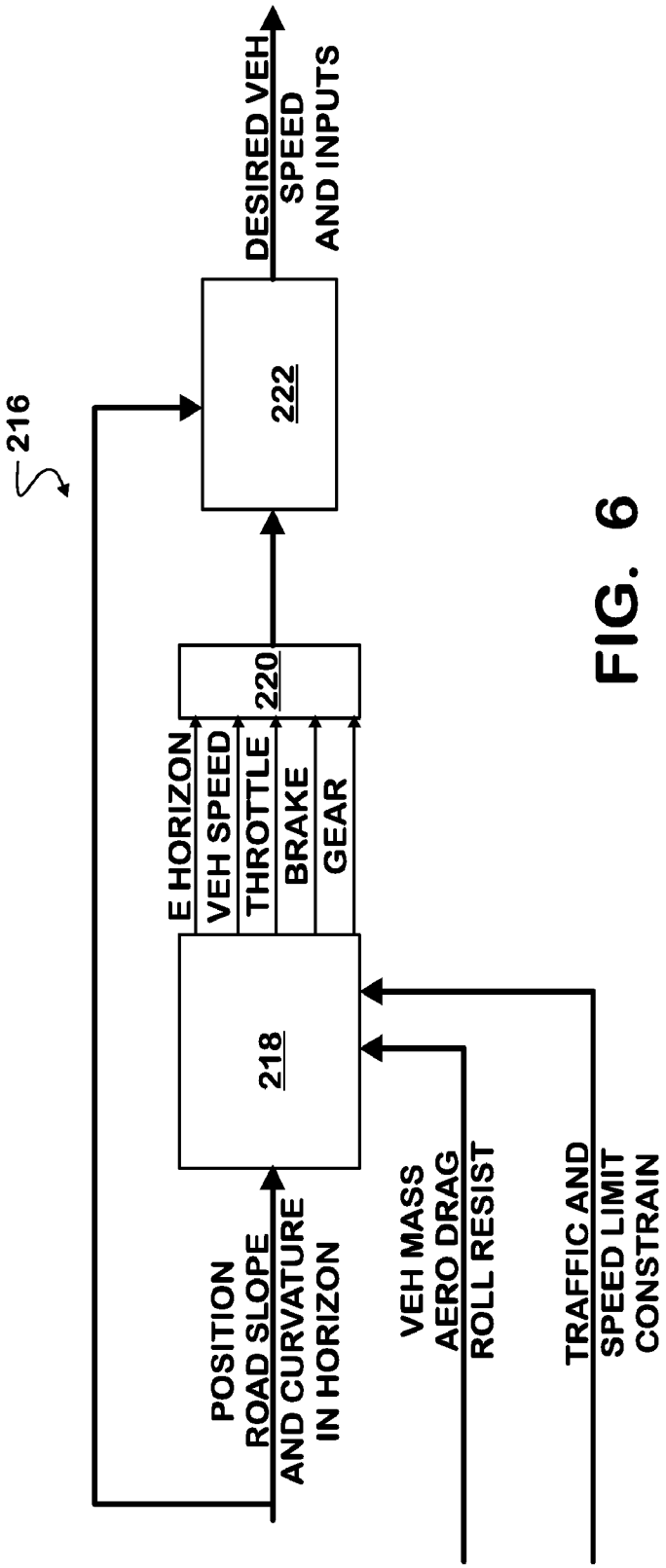
DESIRED VEH SPEED AND INPUTS
222
216
220
E HORIZON
VEH SPEED
THROTTLE
BRAKE
GEAR
218
POSITION ROAD SLOPE AND CURVATURE IN HORIZON
VEH MASS AERO DRAG ROLL RESIST
TRAFFIC AND SPEED LIMIT CONSTRAIN

FIG. 6

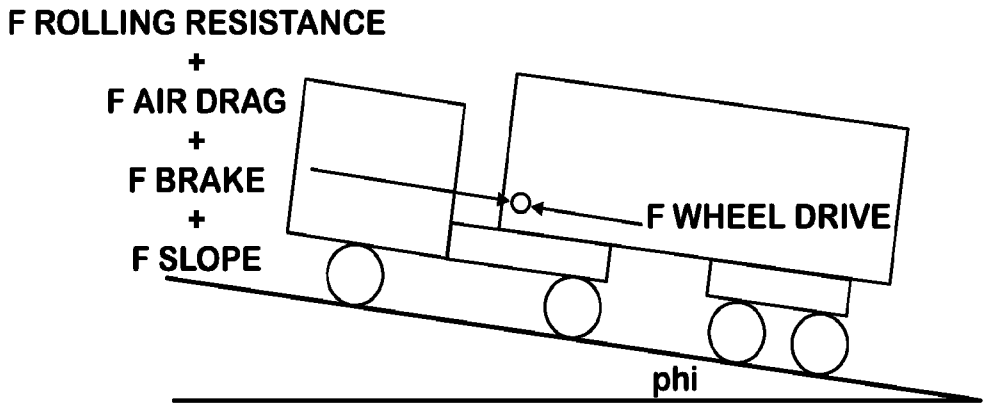
F ROLLING RESISTANCE
+
F AIR DRAG
+
F BRAKE
+
F SLOPE
F WHEEL DRIVE
phi

FIG. 7

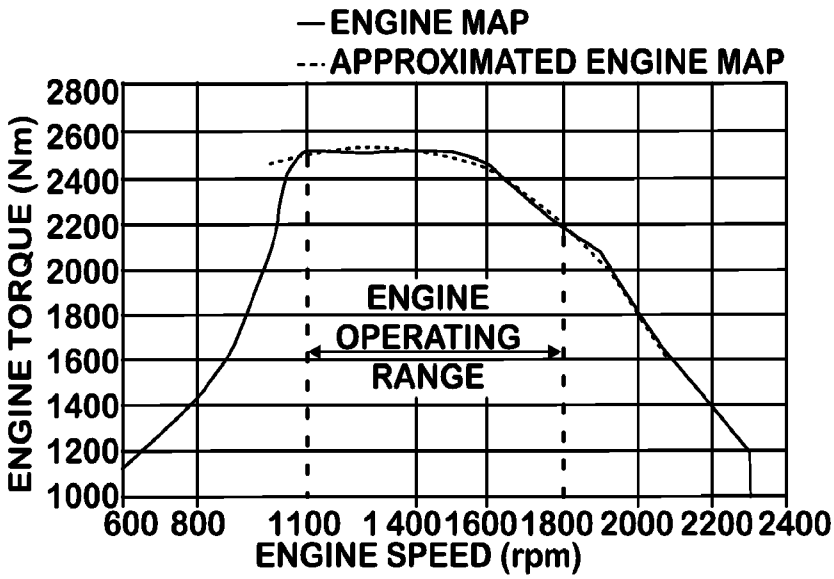
—ENGINE MAP
---APPROXIMATED ENGINE MAP
ENGINE TORQUE (Nm)
2800
2600
2400
2200
2000
1800
1600
1400
1200
1000
ENGINE
OPERATING
RANGE
600 800 1100 1400 1600 1800 2000 2200 2400
ENGINE SPEED (rpm)

FIG. 8

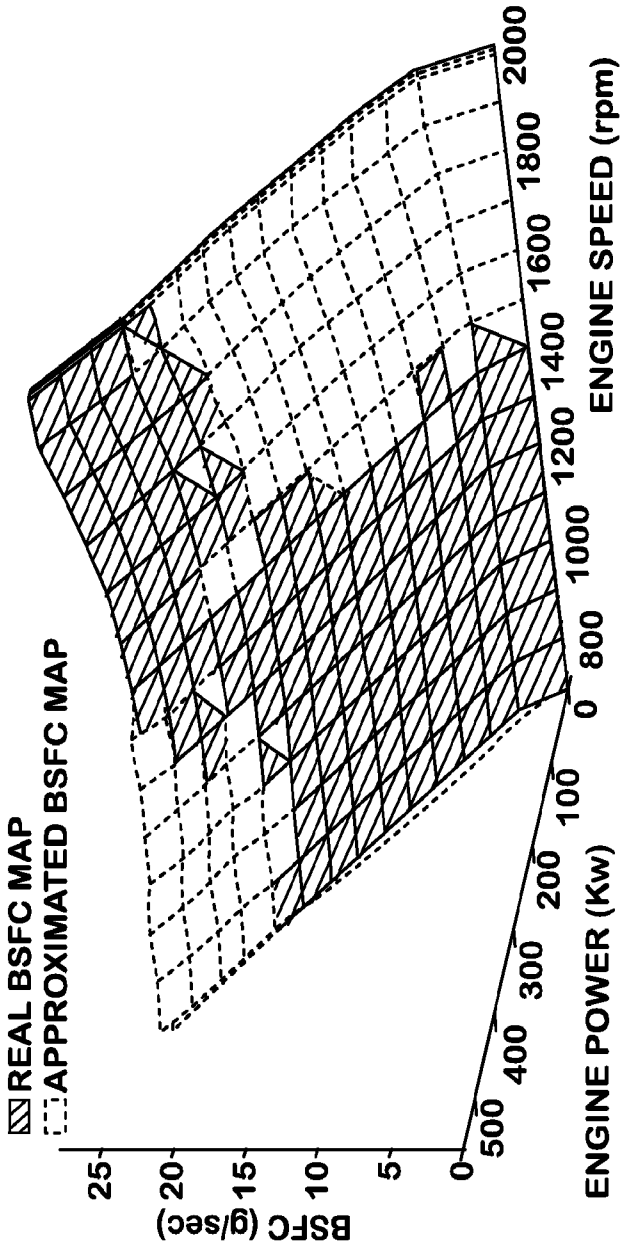
REAL BSFC MAP
APPROXIMATED BSFC MAP
BSFC (g/sec)
25
20
15
10
5
0
ENGINE POWER (Kw)
500
400
300
200
100
0
ENGINE SPEED (rpm)
800
1000
1200
1400
1600
1800
2000

FIG. 9

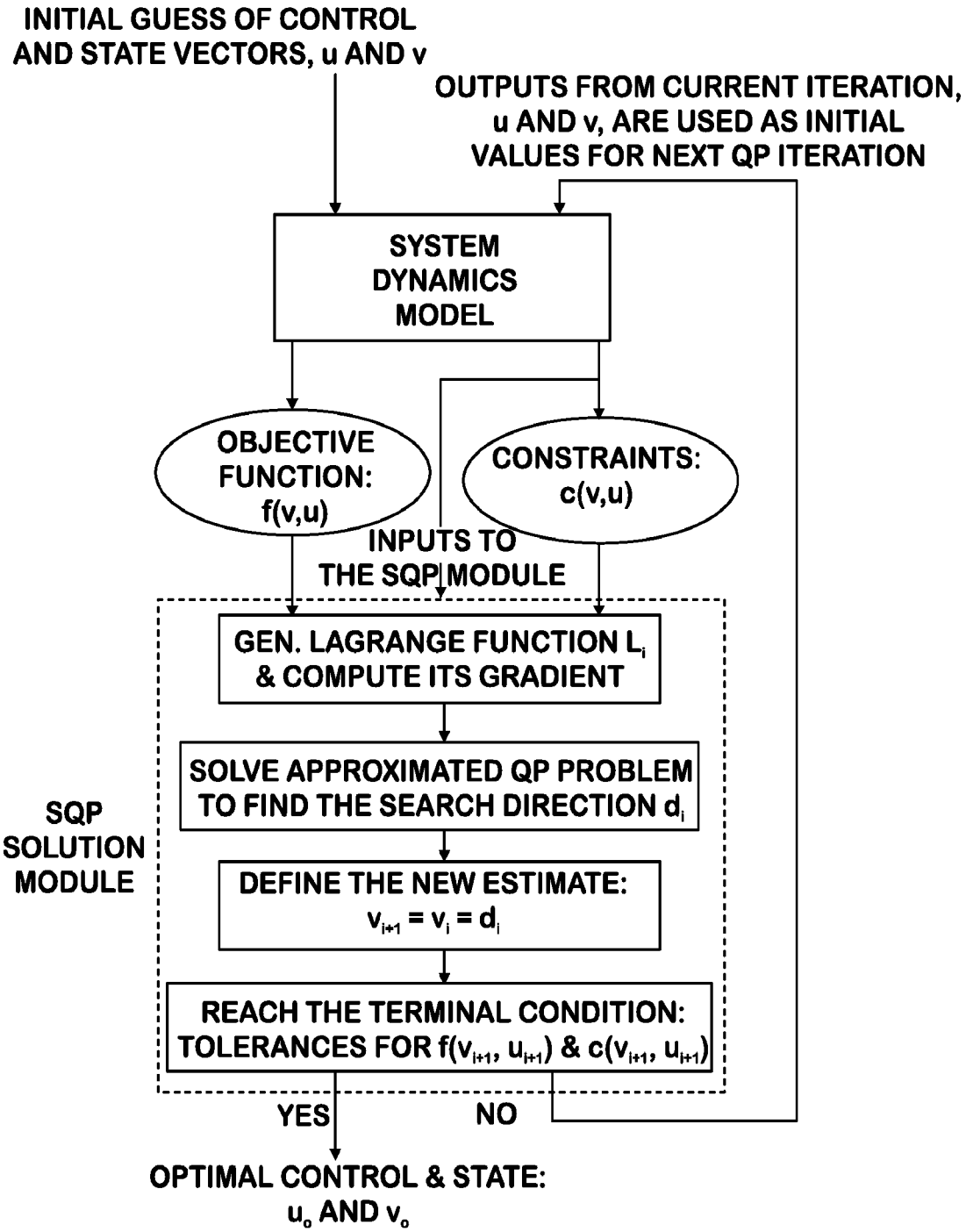
INITIAL GUESS OF CONTROL AND STATE VECTORS, u AND v
OUTPUTS FROM CURRENT ITERATION, u AND v, ARE USED AS INITIAL VALUES FOR NEXT QP ITERATION
SYSTEM DYNAMICS MODEL
OBJECTIVE FUNCTION: f(v,u)
CONSTRAINTS: c(v,u)
INPUTS TO THE SQP MODULE
GEN. LAGRANGE FUNCTION L_i & COMPUTE ITS GRADIENT
SOLVE APPROXIMATED QP PROBLEM TO FIND THE SEARCH DIRECTION d_i
SQP SOLUTION MODULE
DEFINE THE NEW ESTIMATE: $v_{i+1} = v_i = d_i$
REACH THE TERMINAL CONDITION: TOLERANCES FOR $f(v_{i+1}, u_{i+1})$ & $c(v_{i+1}, u_{i+1})$
YES
NO
OPTIMAL CONTROL & STATE: u_o AND v_o

FIG. 10

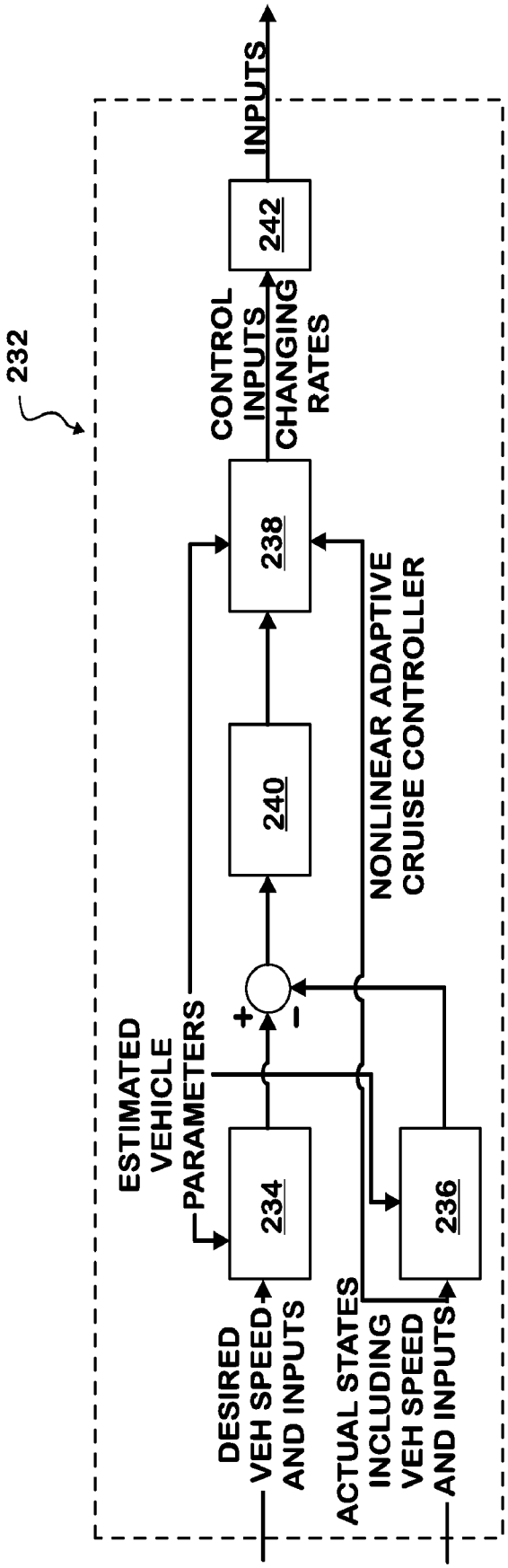
232
DESIRED VEH SPEED AND INPUTS
ACTUAL STATES INCLUDING VEH SPEED AND INPUTS
ESTIMATED VEHICLE PARAMETERS
234
236
+
-
240
238
NONLINEAR ADAPTIVE CRUISE CONTROLLER
CONTROL INPUTS CHANGING RATES
242
INPUTS

FIG. 11

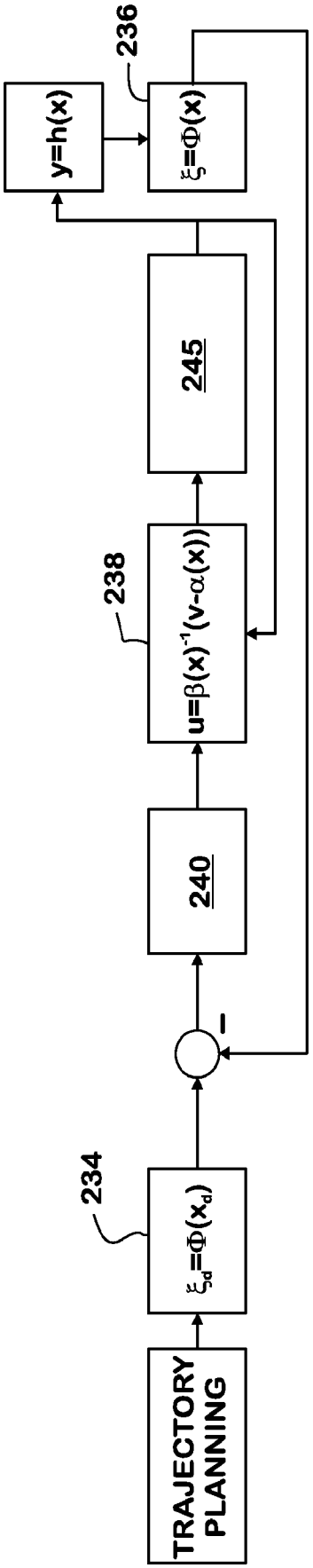
TRAJECTORY PLANNING
234
$\xi_d=\Phi(x_d)$
240
$u=\beta(x)^{-1}(v-\alpha(x))$
238
245
$\xi=\Phi(x)$
236
y=h(x)

FIG. 12

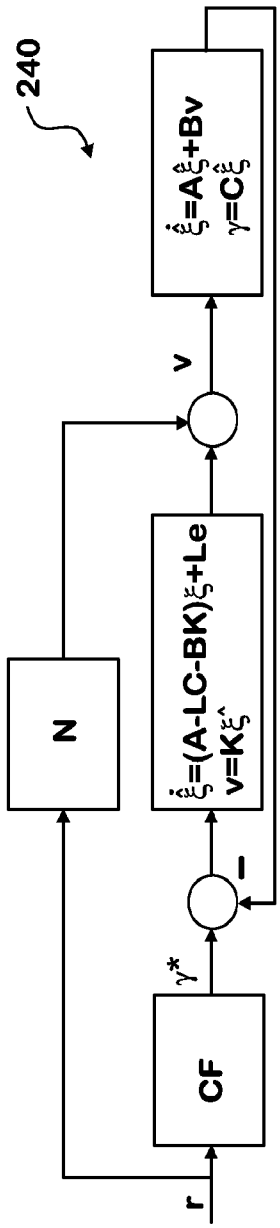
240
N
CF
r
γ^*
$\dot{\hat{\xi}}=(A-LC-BK)\hat{\xi}+Le\gamma$
$v=K\hat{\xi}$
v
$\dot{\hat{\xi}}=A\hat{\xi}+Bv$
$\gamma=C\hat{\xi}$

FIG. 13

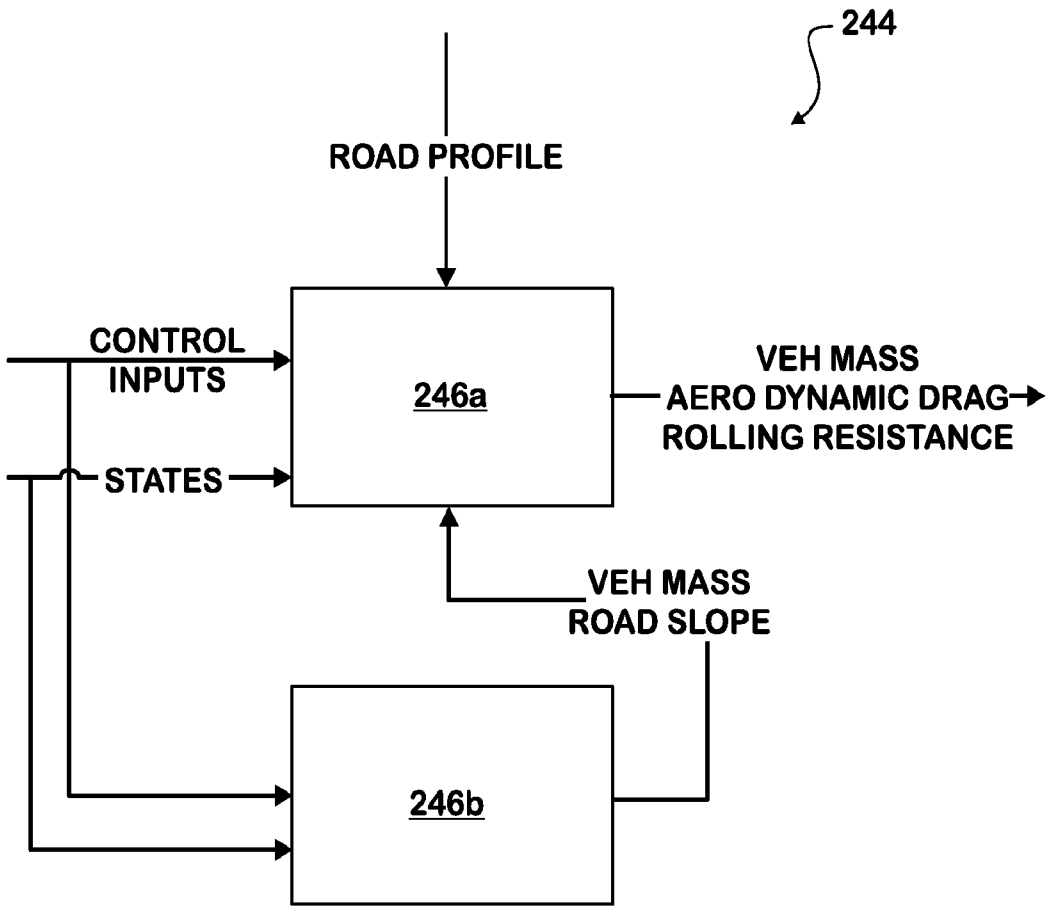
244
ROAD PROFILE
CONTROL INPUTS
STATES
246a
VEH MASS
AERO DYNAMIC DRAG
ROLLING RESISTANCE
VEH MASS
ROAD SLOPE
246b

FIG. 14

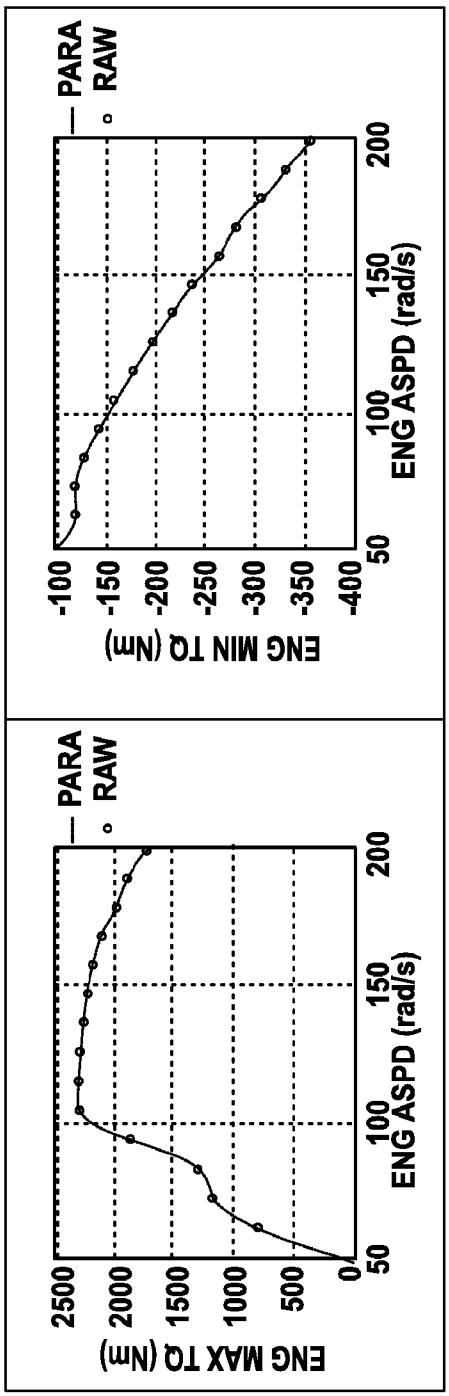
ENG MAX TQ (Nm)
2500
2000
1500
1000
500
0
50
100
150
200
ENG ASPD (rad/s)
— PARA
° RAW
ENG MIN TQ (Nm)
-100
-150
-200
-250
-300
-350
-400
50
100
150
200
ENG ASPD (rad/s)
— PARA
° RAW

FIG. 15

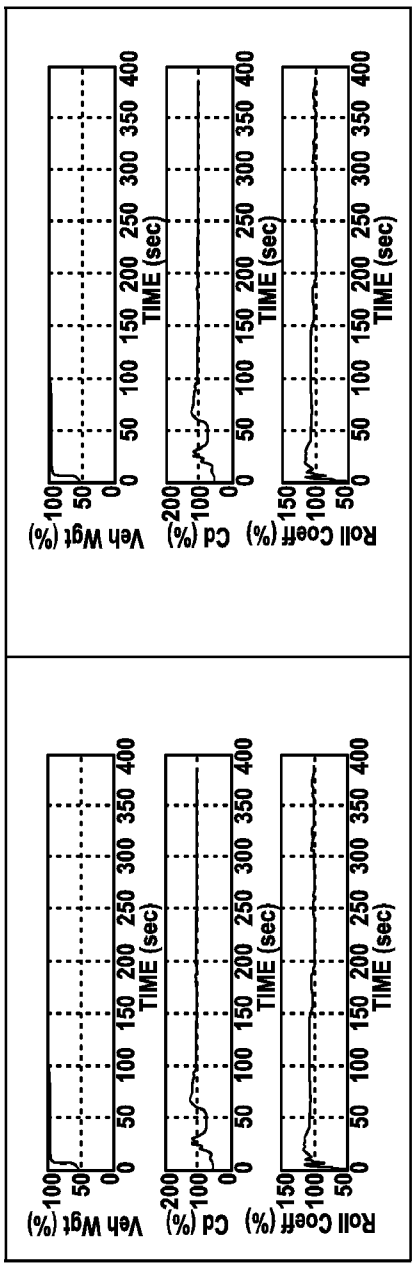
Veh Wgt (%)
100
50
0
0 50 100 150 200 250 300 350 400
TIME (sec)
Cd (%)
200
100
0
0 50 100 150 200 250 300 350 400
TIME (sec)
Roll Coeff (%)
150
100
50
0 50 100 150 200 250 300 350 400
TIME (sec)

FIG. 16

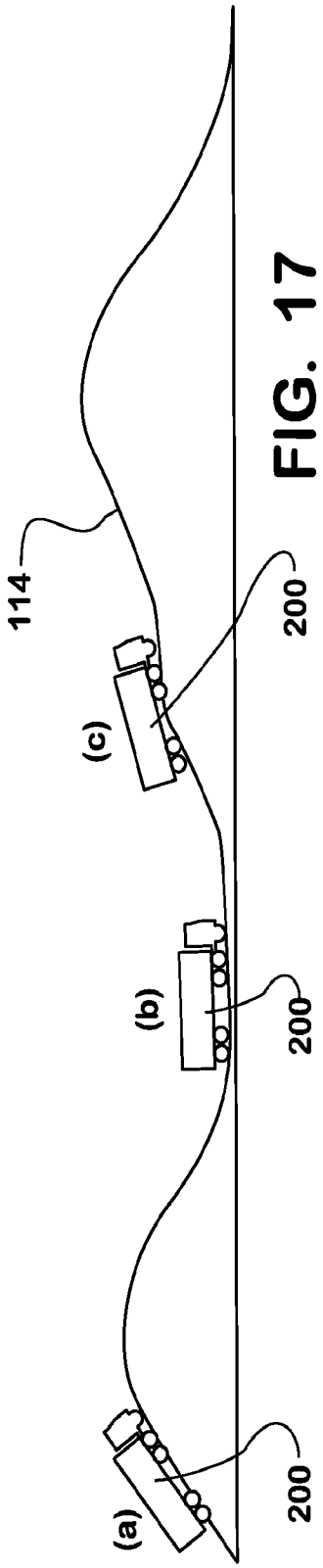

FIG. 17

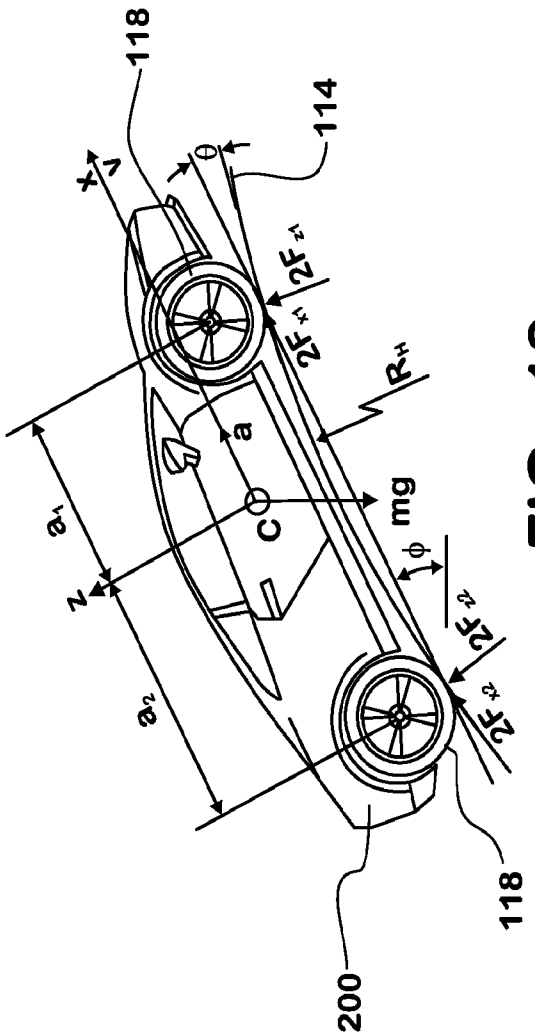

FIG. 18

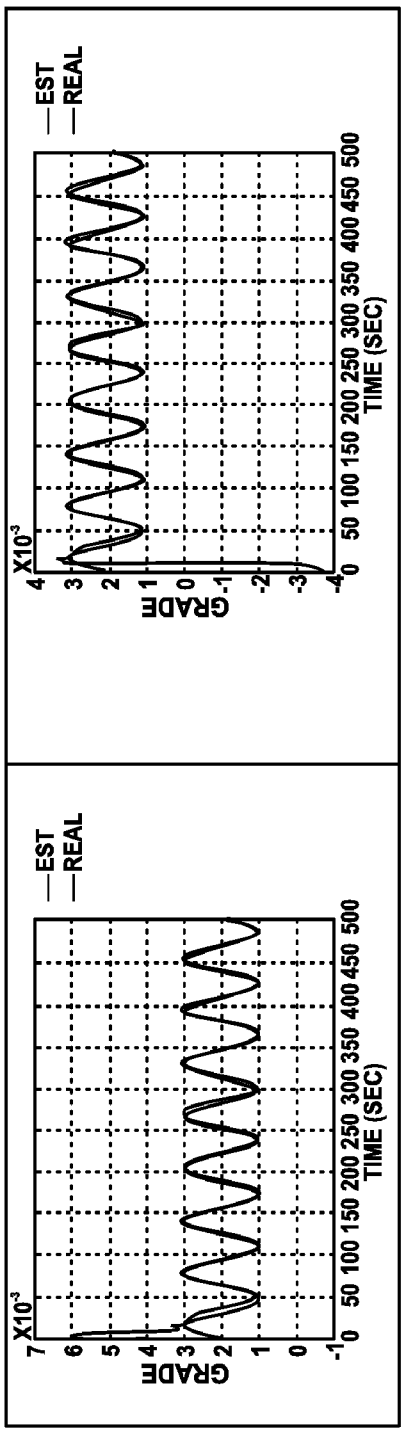
—EST
—REAL
X10-3
GRADE
TIME (SEC)
0 50 100 150 200 250 300 350 400 450 500
7 6 5 4 3 2 1 0 -1
4 3 2 1 0 -1 -2 -3 -4

FIG. 19

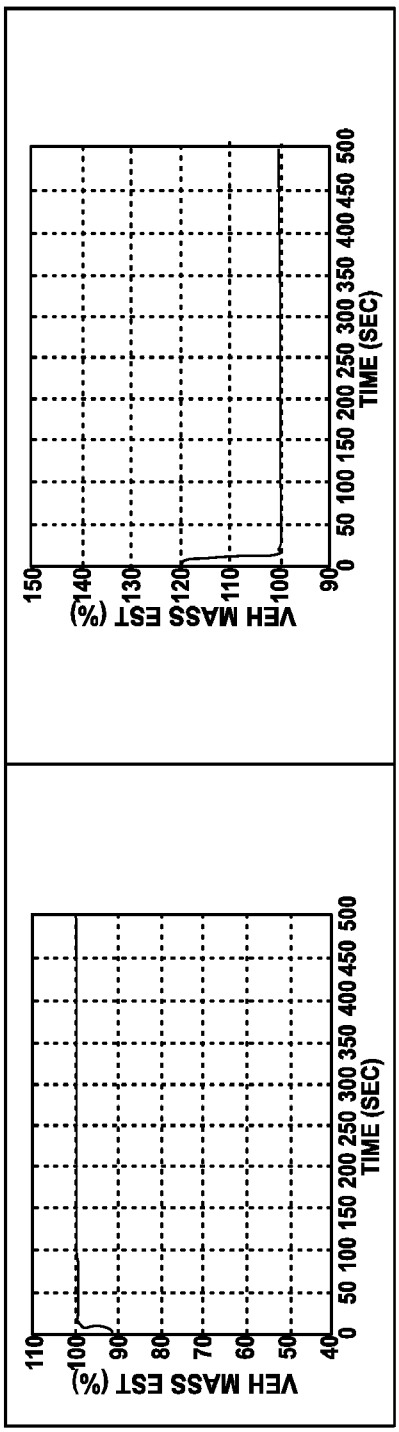
VEH MASS EST (%)
TIME (SEC)
0 50 100 150 200 250 300 350 400 450 500
110 100 90 80 70 60 50 40
150 140 130 120 110 100 90

FIG. 20

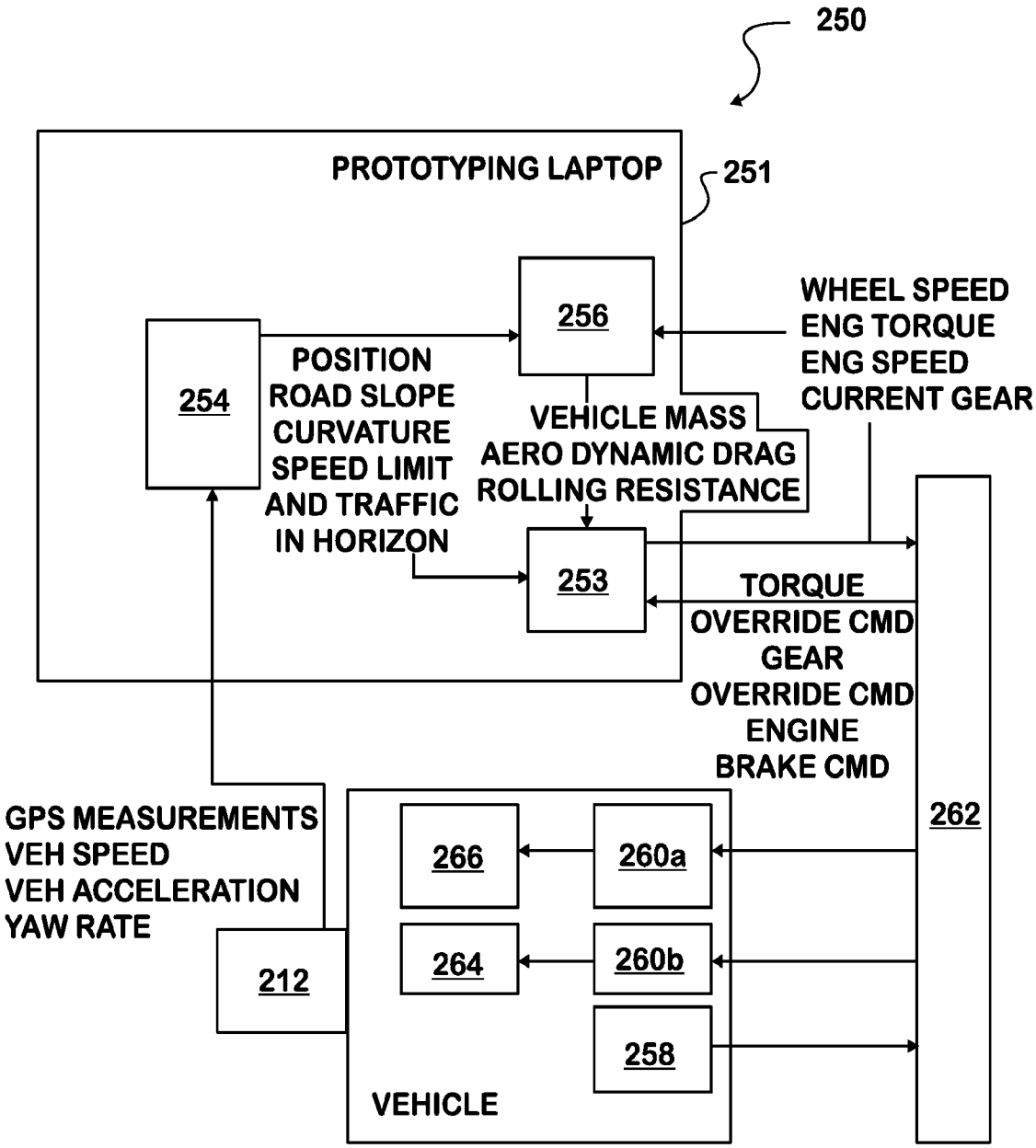
250
PROTOTYPING LAPTOP
251
256
WHEEL SPEED
ENG TORQUE
ENG SPEED
CURRENT GEAR
254
POSITION
ROAD SLOPE
CURVATURE
SPEED LIMIT
AND TRAFFIC
IN HORIZON
VEHICLE MASS
AERO DYNAMIC DRAG
ROLLING RESISTANCE
253
TORQUE
OVERRIDE CMD
GEAR
OVERRIDE CMD
ENGINE
BRAKE CMD
262
GPS MEASUREMENTS
VEH SPEED
VEH ACCELERATION
YAW RATE
266
260a
264
260b
212
258
VEHICLE

FIG. 21

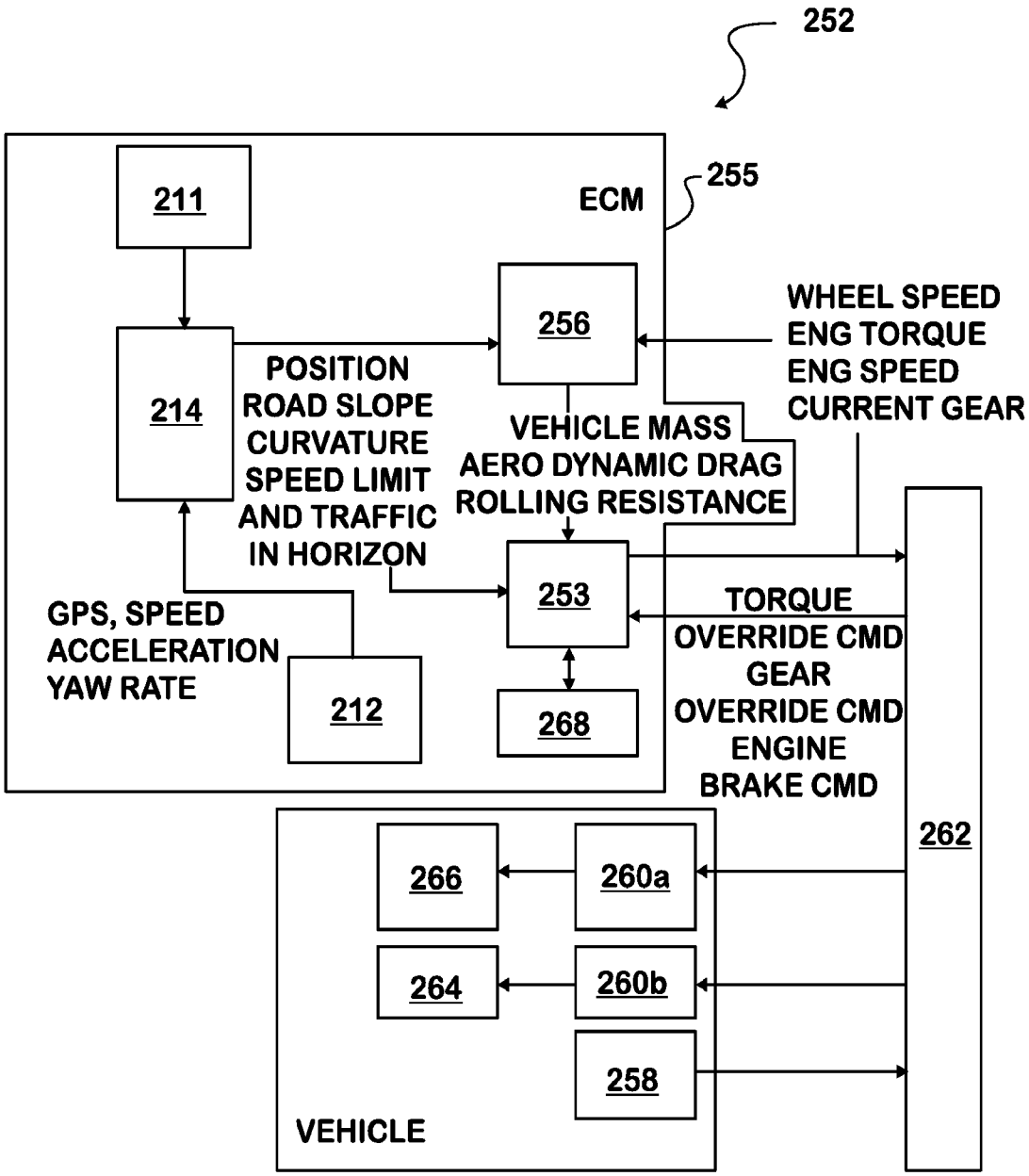
252
ECM
255
211
214
256
253
212
268
262
266
260a
264
260b
258
VEHICLE
WHEEL SPEED
ENG TORQUE
ENG SPEED
CURRENT GEAR
POSITION
ROAD SLOPE
CURVATURE
SPEED LIMIT
AND TRAFFIC
IN HORIZON
VEHICLE MASS
AERO DYNAMIC DRAG
ROLLING RESISTANCE
GPS, SPEED
ACCELERATION
YAW RATE
TORQUE
OVERRIDE CMD
GEAR
OVERRIDE CMD
ENGINE
BRAKE CMD

FIG. 22

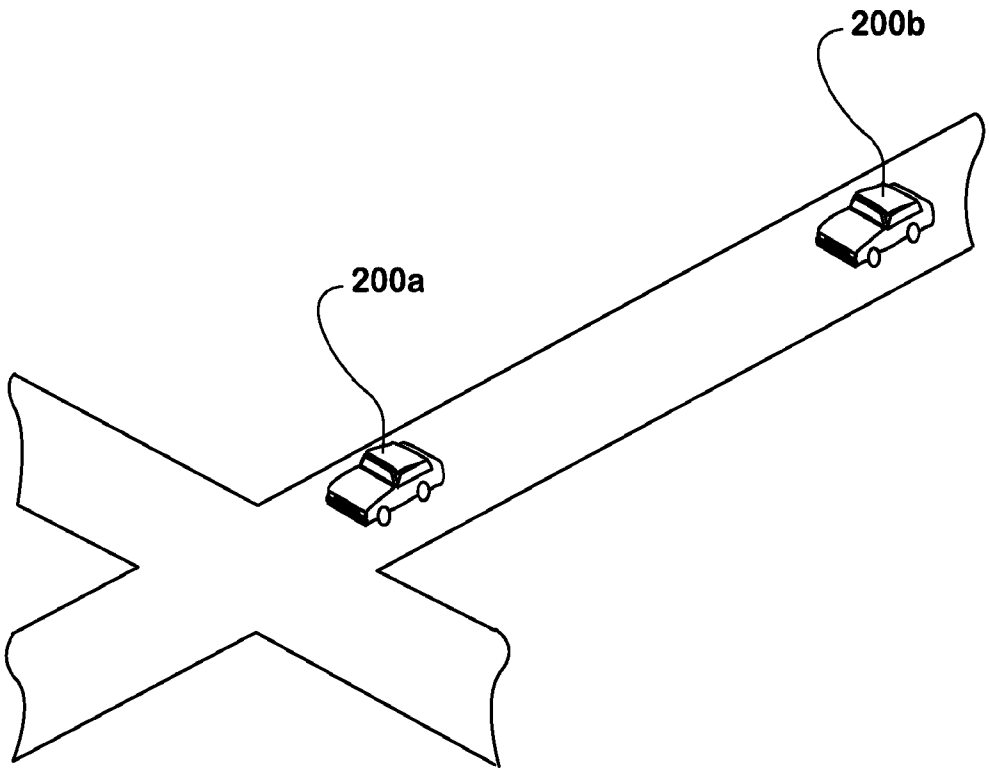

FIG. 23

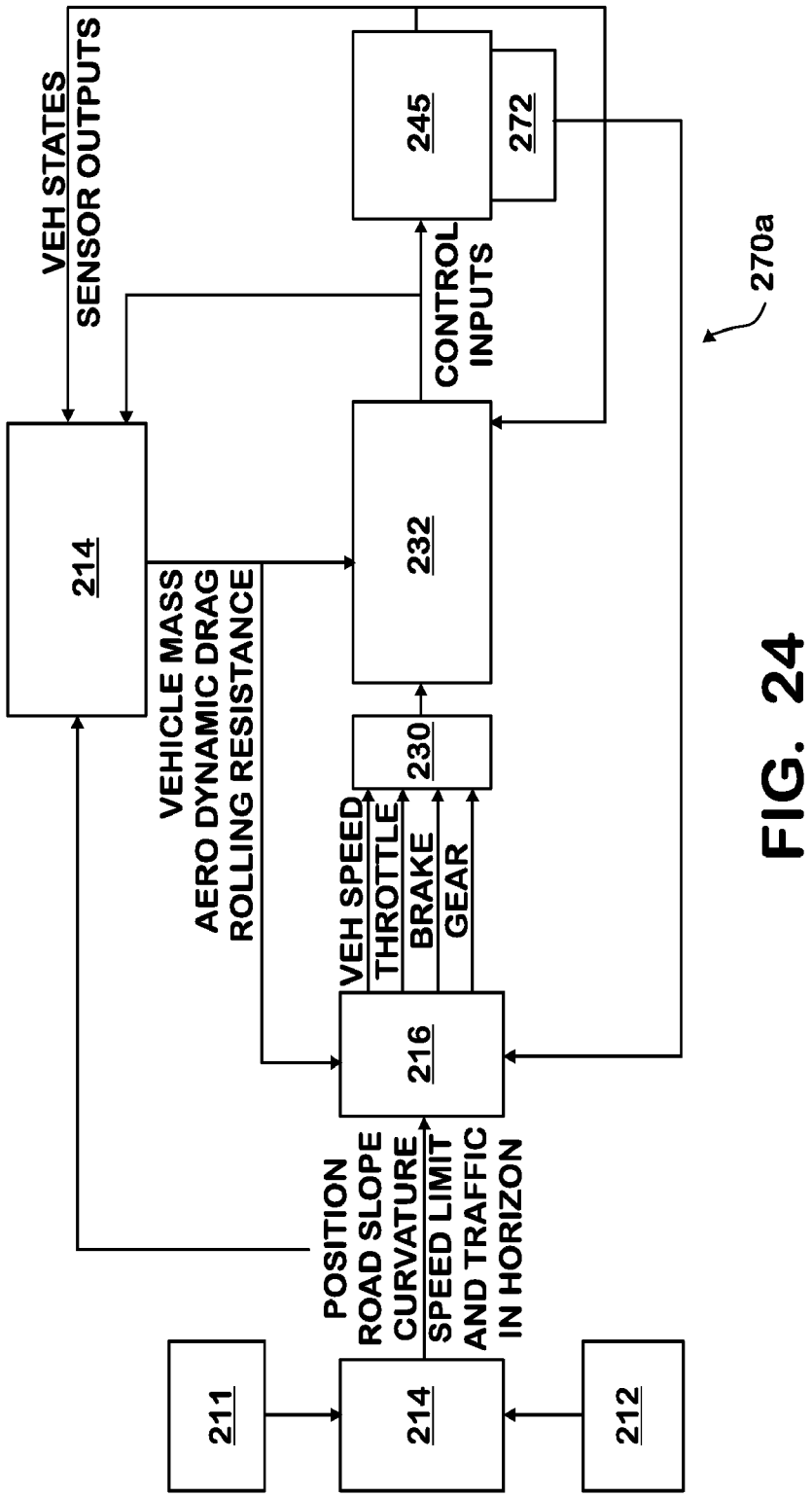
VEH STATES
SENSOR OUTPUTS
245
272
270a
CONTROL
INPUTS
214
232
VEHICLE MASS
AERO DYNAMIC DRAG
ROLLING RESISTANCE
230
VEH SPEED
THROTTLE
BRAKE
GEAR
216
POSITION
ROAD SLOPE
CURVATURE
SPEED LIMIT
AND TRAFFIC
IN HORIZON
211
214
212

FIG. 24

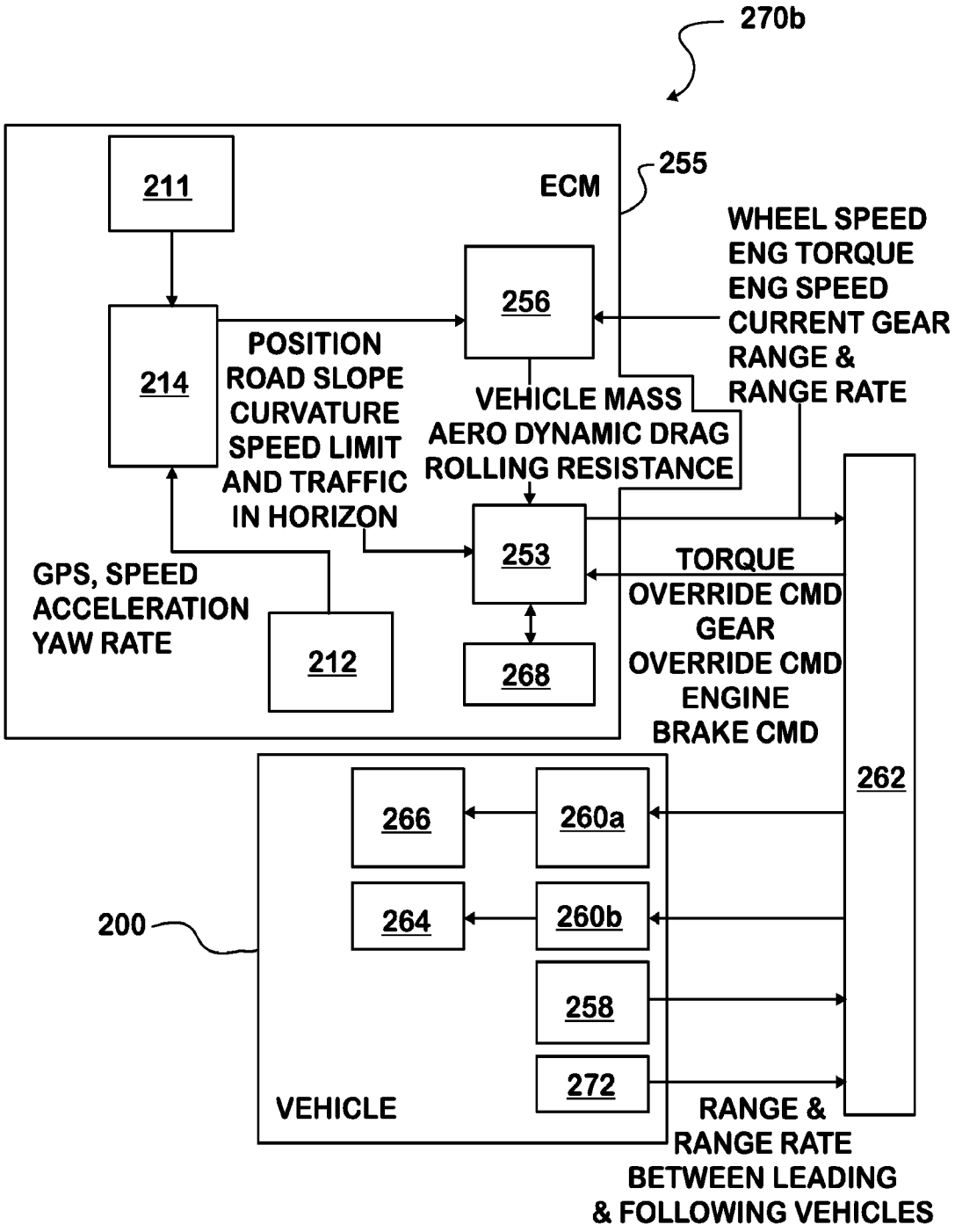
270b
211
ECM
255
WHEEL SPEED
ENG TORQUE
ENG SPEED
CURRENT GEAR
RANGE &
RANGE RATE
256
214
POSITION
ROAD SLOPE
CURVATURE
SPEED LIMIT
AND TRAFFIC
IN HORIZON
VEHICLE MASS
AERO DYNAMIC DRAG
ROLLING RESISTANCE
253
GPS, SPEED
ACCELERATION
YAW RATE
212
268
TORQUE
OVERRIDE CMD
GEAR
OVERRIDE CMD
ENGINE
BRAKE CMD
262
266
260a
264
260b
200
258
272
VEHICLE
RANGE &
RANGE RATE
BETWEEN LEADING
& FOLLOWING VEHICLES

FIG. 25

INTERNATIONAL SEARCH REPORT

International application No.
PCT/US13/33142

A. CLASSIFICATION OF SUBJECT MATTER
IPC(8) - G05D 01/00; G06F 19/00 (2013.01)
USPC - 701/93, 54
According to International Patent Classification (IPC) or to both national classification and IPC

B. FIELDS SEARCHED

Minimum documentation searched (classification system followed by classification symbols)
IPC(8) Classification(s): G05D 01/00; B60W 30/14; B62D 06/00; G06F 19/00 (2013.01)
USPC Classification(s): 701/93, 58, 70, 87, 90, 117, 54

Documentation searched other than minimum documentation to the extent that such documents are included in the fields searched

Electronic data base consulted during the international search (name of data base and, where practicable, search terms used)
MicroPatent (US-G, US-A, EP-A, EP-B, WO, JP-bib, DE-C,B, DE-A, DE-T, DE-U, GB-A, FR-A); DialogPRO; IEEE/IEEEXplore; Google/Google Scholar; IP.com; Search Terms Used: road, surface, condition,characteristic, predict, infer, vehicle, parameter, operation, performance, GPS, inertia, odometer, dead reckoning

C. DOCUMENTS CONSIDERED TO BE RELEVANT

Category*	Citation of document, with indication, where appropriate, of the relevant passages	Relevant to claim No.
X – Y	US 2008/0027612 A1 (ERIKSSON, A et al.) January 31, 2008; abstract, figure 3, paragraphs [0007], [0009], [0017], [0020], [0022]	1-11 --- 12-15
Y	US 2012/0323474 A1 (BREED, D et al.) December 20, 2012; paragraphs [0022], [0023], [0027]-[0029], [0035], [0117], [0119], [0430]	12-15

☐ Further documents are listed in the continuation of Box C. ☐

* Special categories of cited documents:
"A" document defining the general state of the art which is not considered to be of particular relevance
"E" earlier application or patent but published on or after the international filing date
"L" document which may throw doubts on priority claim(s) or which is cited to establish the publication date of another citation or other special reason (as specified)
"O" document referring to an oral disclosure, use, exhibition or other means
"P" document published prior to the international filing date but later than the priority date claimed
"T" later document published after the international filing date or priority date and not in conflict with the application but cited to understand the principle or theory underlying the invention
"X" document of particular relevance; the claimed invention cannot be considered novel or cannot be considered to involve an inventive step when the document is taken alone
"Y" document of particular relevance; the claimed invention cannot be considered to involve an inventive step when the document is combined with one or more other such documents, such combination being obvious to a person skilled in the art
"&" document member of the same patent family

Date of the actual completion of the international search	Date of mailing of the international search report
3 June 2013 (03.06.2013)	19 JUN 2013
Name and mailing address of the ISA/US Mail Stop PCT, Attn: ISA/US, Commissioner for Patents P.O. Box 1450, Alexandria, Virginia 22313-1450 Facsimile No. 571-273-3201	Authorized officer: Shane Thomas PCT Helpdesk: 571-272-4300 PCT OSP: 571-272-7774

Form PCT/ISA/210 (second sheet) (July 2009)